Development of HPLC-FID Coupling Using Water as the Eluent

by

Rui Zhang

A thesis

presented to the University of Waterloo

in fulfillment of the

thesis requirement for the degree of

Master of Science

in

Chemistry

Waterloo, Ontario, Canada, 2010

Author's Declaration

I hereby declare that I am the sole author of this thesis. This is a true copy of the thesis, including any required final revisions, as accepted by my examiners.

I understand that my thesis may be made electronically available to the public.

Abstract

The characterization of all components of pharmaceutical preparations, especially in the analysis of impurities present at levels higher than 0.05% of the main component, is a challenge in the pharmaceutical industry because no single detector can detect all impurities present. All commercial detection methods suffer from certain disadvantages. Universal sensitive detection with a wide dynamic range is strongly demanded. This results in an increasing interest in the development of universal sensitive detection methods for the pharmaceutical industry, which was the goal of this project.

In this project, universal detection of analytes by HPLC-FID coupling was explored. Due to the large volume of the vapours of the mobile phase in HPLC, flame-based detection systems are prone to flame instability. To overcome this problem, a series of improvements were evaluated: 1) a fraction of the total volume of the effluent was delivered to the flame of the FID in a split mode; 2) a tubular oven was used before the FID to preheat the effluent and remove a large fraction of the mobile phase before the detector; 3) oxygen gas and a modified FID with an elongated burner were used to improve the performance of the FID. Finally, optimization of the FID design and parameters was performed by running a series of tests in flow injection mode using simplex optimization method.

Acknowledgement

I would like to express my gratitude to all who have helped me in the completion of this project. First of all, I would like to thank my supervisor, Dr Tadeusz Górecki for giving the opportunity to work on this challenging project, also for his encouragement and guidance during the whole period of research. Secondly, I would like to thank my advisory committee members, Dr. Jean Duhamel and Dr. Wojciech Gabryelski for their patience and valuable advice.

I would also like to thank my colleagues in our group, both those who are still working hard in the lab and those who have graduated. Their help and suggestions made the research work a lot easier. Their efforts are greatly recognized.

Finally, I would like to thank my family and friends, for their understanding and supporting me, and helping me go through the most difficult days of my research work.

Table of Contents

List of Figures

List of Tables

List of Abbreviation

APCI	Atmospheric Pressure Chemical Ionization
CLND	Chemiluminescent Nitrogen Detector
ELSD	Evaporative Light Scattering Detector
ESI	Electrospray Ionization
FID	Flame Ionization Detector
FIA	Flow Injection Analysis
HPLC	High Performance Liquid Chromatography
^{1}H-NMR	Proton Nuclear Magnetic Resonance
LOD	Limit of Detection
MS	Mass Spectrometry
m/z	mass-to-charge ratio
mp	melting point
ODS	Octadecylsilyl
ppm	parts per million
PS/DVB	Polystyrene/divinylbenzene
RID	Refractive Index Detector
RP-HPLC	Reversed Phase High Performance Liquid Chromatography
SHWC	Superheated Water Chromatography
UV	Ultraviolet
μLC	Micro-column Liquid Chromatography

Chapter 1.0

1.1 Introduction

Chromatography was invented by Russian botanist Mikhail Semyonovich Tswett at the beginning of the last century during his research on chlorophyll. A century later, chromatography is being applied in many different ways. The goal of this technique is to obtain quantitative or/and qualitative chemical information about mixtures of interest by separating and detecting their components.

A typical analytical process consists of sampling, sample preparation, separation and detection. Sample preparation plays an important role in concentrating and extracting the analyte(s) from matrix interferences in order to avoid problems during the detection stage. Depending on the type of application, purified samples are separated by a suitable chromatographic method. Finally, a sensitive detector collects information on the analytes leaving the separation system.[1]

High performance liquid chromatography (HPLC) is one of the most widely used analytical separation techniques in the pharmaceutical, environmental, forensic, clinical, and food and fragrance sectors, among others. It is the most reliable method for analyzing non-volatile organic compounds. The instrumental components of an HPLC system are illustrated in **Figure 1-1**. In principle, HPLC is an elution process using constant mobile phase composition or solvent gradient. The analyte is introduced in a small volume to the stream of the mobile phase, and then is forced through the stationary phase, which separates the sample components by the difference in their retention times. Separation of analytes takes place in a column packed with regularly shaped particles or a porous monolithic stationary phase. It is driven by the partitioning of sample components between the mobile phase and the stationary phase.[1]

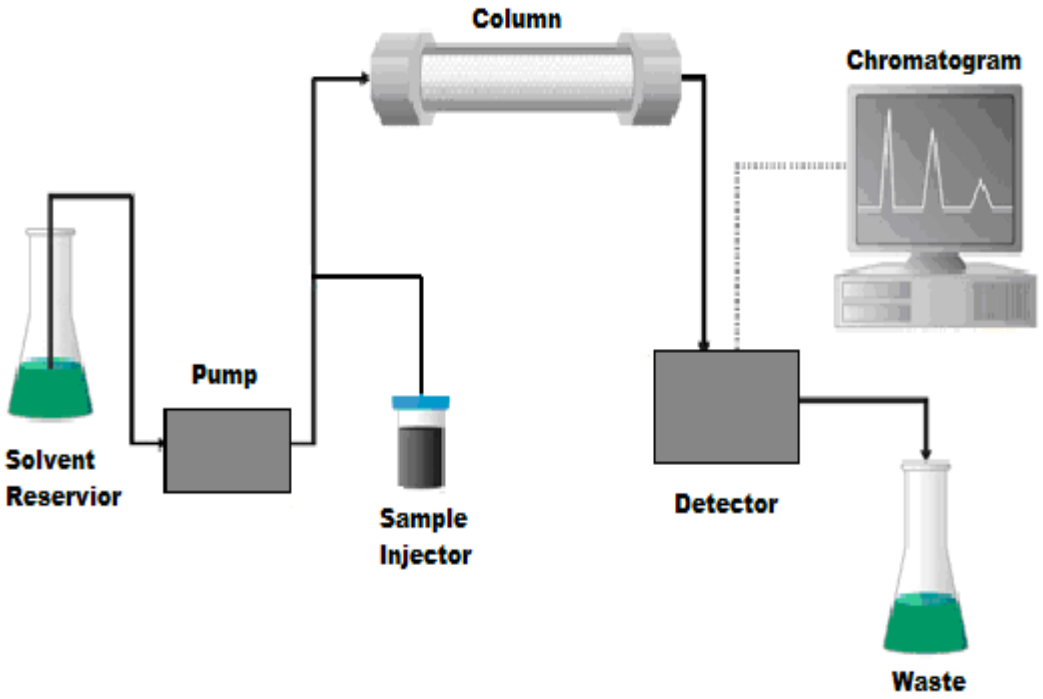

Figure 1-1. General schematic of a commercial HPLC[2]

Ideally, all sample components eluting from the column are detected by a suitable detector. The plot of detector signal vs. time generates a so-called chromatogram, which represents the separated analytes as peaks characterized by signal intensity and retention time. In reality, however, some components of complex samples often cannot be detected efficiently using typical HPLC detectors. This is a particularly severe problem in the pharmaceutical industry, where all components of pharmaceutical preparations (including impurities present at levels higher than 0.05 % of the main component) must be characterized.

1.2 Detection in HPLC

Several typical detectors used in HPLC are described below: ultraviolet (UV), refractive index (RID), evaporative light scattering (ELSD), chemiluminescent nitrogen

(CLND), electrochemical, fluorescent and mass spectrometric (MS) detectors. The advantages and drawbacks of them are briefly discussed. Some of their important properties are listed in **Table 1-1**.

Table 1-1. Comparison of commercial HPLC detectors.[1]

Detector	Approximate limit of detection (ng)	Useful with gradient?
Ultraviolet	0.1-1	Yes
Refractive index	100-1000	No
Evaporative light-scattering	0.1-1	Yes
Electrochemical	0.01-1	No
Fluorescence	0.001-0.01	Yes
Chemiluminescent nitrogen	0.3	Yes
Conductivity	0.5-1	No
Mass spectrometry	0.1-1	Yes
Fourier transform infrared	1000	Yes

1.2.1 UV Detection

UV/visible is the dominant detection mode in HPLC due to its low cost and versatility. A typical UV detector in HPLC uses a flow cell as shown in **Figure 1-2**. Principally, the utility of UV detectors is based on the capacity of compounds to absorb light in the range of wavelengths from 190 to 350 nm.[1] UV detection can be carried out at one or more wavelengths. There are three basic types of UV detectors: fixed wavelength, variable wavelength and diode array. Fixed wavelength detectors measure absorption at a single wavelength only, usually 254 nm; variable wavelength detectors measure absorption at one wavelength at a time over a wide range of selectable wavelengths; diode array detectors measure an entire spectrum of wavelengths simultaneously. According to Beer's law, UV detectors measure changes in absorbance of light expressed as the ratio of

the intensity of an incident beam (I_0) and the intensity of radiation emerging from the sample (I). In a simple system, a monochromator and a lamp such as mercury, deuterium, xenon or tungsten are used. A limit of detection (LOD) of 0.1 ng is achievable (see **Table 1-1**). The linear range extends over five orders of magnitude of solute concentrations.[1] The drawback of this detection method is that it is only sensitive to compounds containing chromophores.

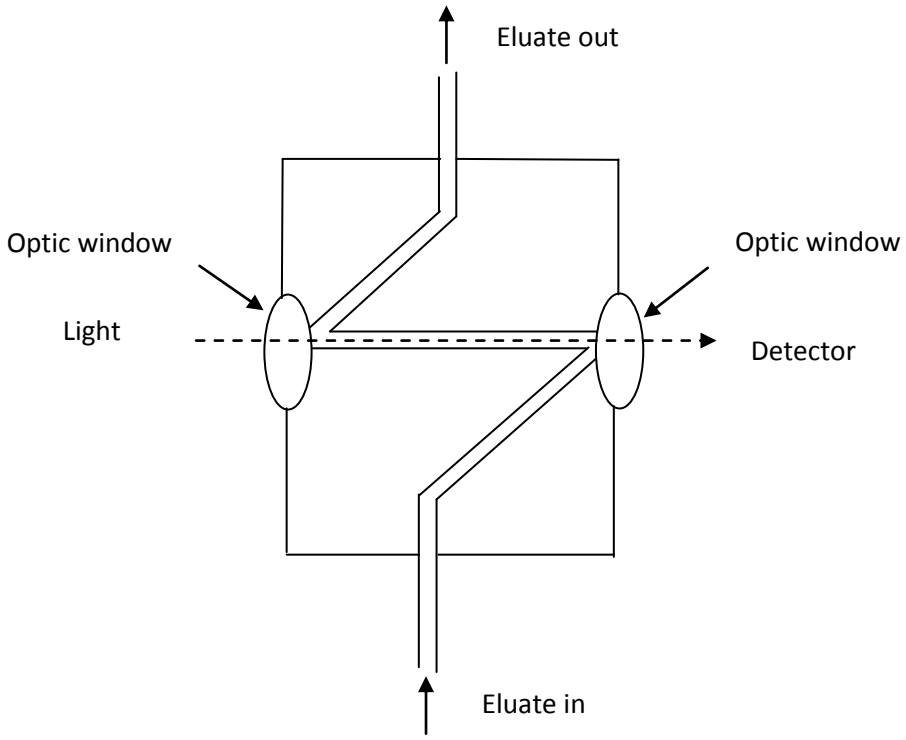

Figure 1-2. Light path in a spectrophotometric flow cell (Based on reference 1).

1.2.2 RI Detection

RI detectors have the significant advantage of responding to nearly all solutes. They measure the ability of sample molecules to refract light based on their refractive indices. In a typical RI detector, light passes through a bi-compartment flow-cell to a photocell. The eluate flows through one channel of the flow-cell, while only the mobile phase (reference) flows through the second channel. Detection occurs when the light is bent due to presence of a solute with a refractive index different from that of the mobile phase. This disparity between two channels with respect to the photosensitive surface of a detector causes variation in the output signal, which is shown as the chromatogram[1]. Although refractive index detectors are universal in theory, they are not suitable for gradient elution, since the sample and the reference cannot match exactly during the change of solvent composition. More importantly, their detection limits are only 100-1000 ng, about 1000 times poorer than those of UV detectors (see **Table 1-1**). Consequently, they are not useful for trace analysis. They also have a narrow linear range (a factor of 500 in solute concentration) and are highly sensitive to temperature and pressure variations.[1]

1.2.3 Evaporative Light Scattering Detection

An evaporative light-scattering detector (ELSD) can detect any analyte that is significantly less volatile than the mobile phase, independently of the analyte's optical electrochemical or other properties. ELSD can therefore offer distinct advantages in gradient separation compared to conventional UV or RI detection. The basic mechanism of ELSD detection consists of three stages: 1) nebulization, 2) mobile phase evaporation, 3) detection. During the nebulization stage, the mobile phase is forced through a fine

nozzle with a flow of nitrogen or air to form an aerosol plume containing a uniform dispersion of droplets.

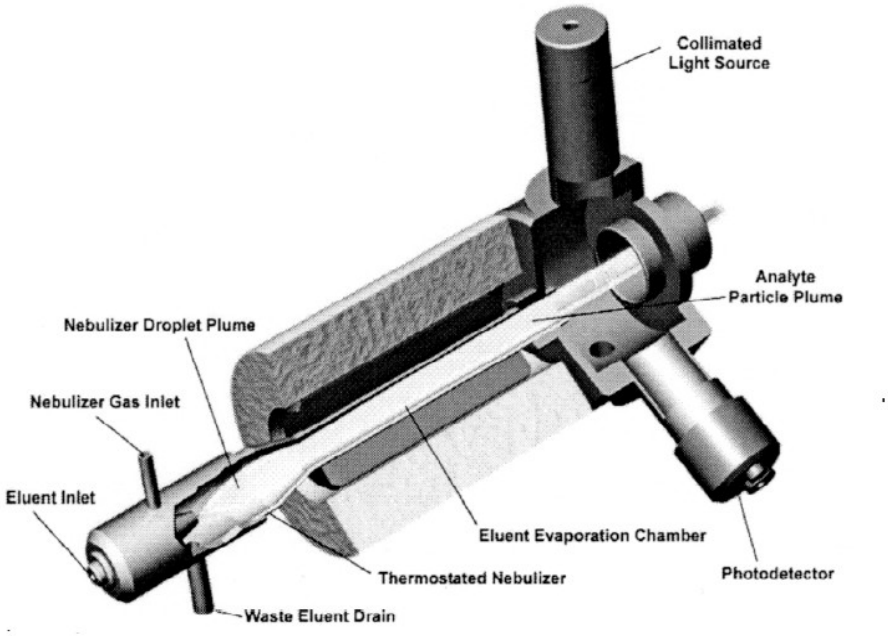

Figure 1-3. Cross-section of an ELS detector[3]

The aerosol then enters a heated coil or tube where volatile components and solvents are evaporated, leaving residual particles of the analyte. The remaining analyte particles are irradiated by a light source. Light scattered by the particles is detected by a photomultiplier or a photodiode (see **Figure 1-3**).[4,5] ELSD is more sensitive than the RI detector and compatible with gradient elution (see **Table 1-1**). However, there are still some weaknesses in this type of detection: 1) ELSD has limited sensitivity. 2) its response is non-linear between mass and signal intensity, and depends strongly on the mobile phase composition. Higher contents of organic modifiers in the mobile phase result in higher response; 3) this detection mode is also affected by analyte melting point (mp). Some analytes cannot be distinguished from the volatilized mobile phase

background when the ELSD temperature is higher than the mp of the compound of interest. Consequently, ELSD falls short of being a true "universal detector".[6]

1.2.4 Chemiluminescent Nitrogen Detection (CLND)

The chemiluminescent nitrogen detector (CLND) is a nitrogen-specific detector that produces a linear response to chemically bonded nitrogen atoms in organic compounds. In a typical CLND, oxidation of the column effluent in a high temperature furnace converts all nitrogen-containing compounds into nitric oxide. The resulting dried gas is mixed with ozone in a reaction chamber to form excited-state nitrogen dioxide (NO_2^*), which instantaneously relaxes to its ground state with a resulting emission of chemiluminescent light. The emitted light is detected by a photomultiplier and is proportional to the moles of nitrogen present in the sample. Because of its high sensitivity (see **Table 1-1**) and selectivity, CLND is very useful in the analysis of pharmaceuticals provided that they contain nitrogen. However, all mobile phase components containing nitrogen cause baseline noise and cannot be used (e.g. acetonitrile).[7]

1.2.5 Electrochemical/ Fluorescence Detectors

Both of these detectors provide high sensitivity, but also high selectivity. In particular, electrochemical detectors measure only compounds with active functional groups that can be oxidized or reduced; fluorescence detectors measure analytes that fluoresce.[1] To increase the utility of both types of detectors, derivatization might be performed by adding reagents that modify the analytes.[8] Nevertheless, these detectors cannot be treated as universal.

1.2.6 MS Detection

Mass spectrometry is desirable as a powerful detection technique for any type of separation. However, the LC-MS coupling proved to be much more difficult than the GC/MS coupling due to the large volume of the vapors of the liquid mobile phase. Because high liquid flows from HPLC were not compatible with the high vacuum required by the mass spectrometer, an interface had to be added between the LC and the MS. Several types of interfaces have been investigated, including thermospray,[9] particle beam interface, electrospray ionization (ESI),[10,11] and atmospheric pressure chemical ionization (APCI).[12] APCI and ESI techniques are now the methods of choice for many LC-MS applications. The general mechanism of MS is that the sample is ionized and then passed through a mass analyzer (typically a simple quadrupole), where the ions formed from the analyte molecules are separated according to their mass-to-charge ratio (m/z).[1] Although it is well known that MS is a spectroscopic technique with high sensitivity (0.1-1 ng) and reliability, it does not qualify as a truly universal detection method. Only ionized molecules eluting from the column can be detected, and none of the currently used methods are capable of ionizing all analytes.

1.3 Fundamentals of Superheated Water Chromatography (SHWC)

1.3.1 The Principle of SHWC

Most analyses in reversed-phase high performance liquid chromatography are carried out in isothermal mode around ambient temperature (up to 35 °C) with gradient elution.[13] Water is used to reduce the elution strength of the stronger non-polar organic modifiers and is a poor solvent for most organic compounds. Temperature is often

considered a parameter that has no or little effect on separation quality. However, when the temperature is increased to anywhere between 100 °C and 250 °C under sufficient pressure, the permittivity (dielectric constant), surface tension, and viscosity of liquid water change markedly and approach those of water-organic solvent mixtures at room temperature, so that water can be used as the sole eluent (see **Figure 1-4**).

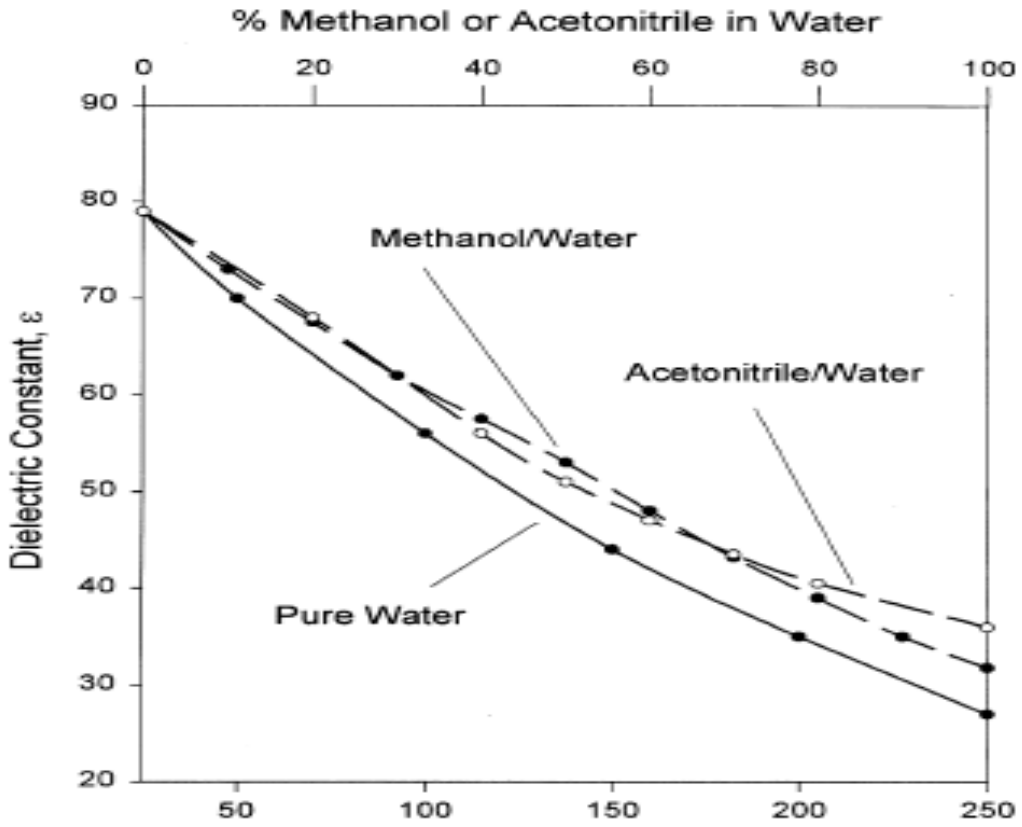

Figure 1-4. The effect of temperature on eluent polarity. Control of eluent polarity (dielectric constant) by changing water temperature (at 50 bar) and by mixing methanol or acetonitrile with water at 25 °C.[14]

For example, the relative permittivity of water at about 200 °C is similar to that of methanol and acetonitrile.[15] As the temperature of water increases, only modest pressure is required to maintain it in a condensed state and to prevent steam formation (see **Figure 1-5**).[16] In addition, the use of elevated temperature reduces viscosity (which also results in

the increase in the solutes' diffusion coefficients) and analysis duration without loss of efficiency. Therefore, SHWC has the potential to significantly improve productivity. Potentially, this is a trend which should be explored further as a way of reducing costs and the use of toxic organic solvents, increasing the versatility of analytical methodologies.

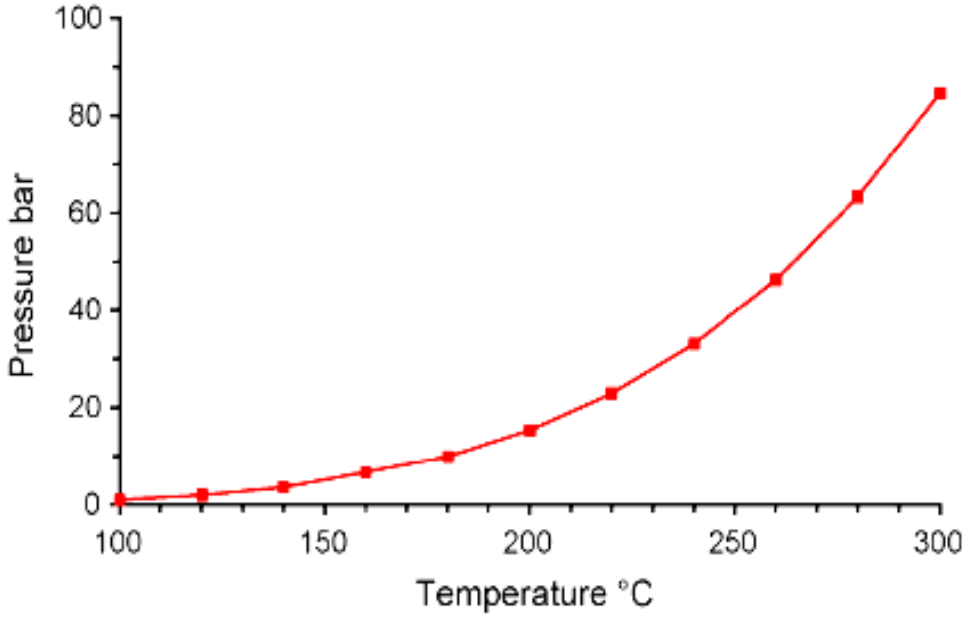

Figure 1-5. Vapor pressure of water at different temperatures.[16]

1.3.2 SHWC Instrumentation

The instrumentation required to carry out SHWC usually is the same as that for conventional HPLC, except for the addition of a column oven and a method of controlling column backpressure (a pressure restrictor). Also, preheating of the mobile phase should be employed to improve the performance of the system.

Column/stationary phase

Column selection plays an important role in the success of any separation. Many of the studies used conventional HPLC column sizes (100-250 mm x 4-4.6 mm I.D. with 3-5 μm particles). Alternatively, because of the low viscosity of water at elevated temperature, the use of small particle sizes or multiple linked columns becomes possible.[17] Takeuchi et al. found that the low mass of narrower bore columns (<1 mm) enabled them to respond rapidly to temperature programming and offered low resistance to thermal transfer.[18] In addition to the effect of column diameter, column packing materials are the other limiting factor. Generally, octadecylsilyl(ODS)-bonded silica phases are widely accepted in conventional ambient temperature HPLC, but they often degrade at temperatures above 100 °C. Due to the poor stability of conventional stationary phases at elevated temperatures, thermally stable stationary phases have been developed and proposed (see **Table 1-2**). Commercial column materials used for SHWC include silica, polymer, and zirconia-based columns.

Table 1-2. Commercially available columns for SHWC

Column materials	Stationary phase	Temperature Limit (°C)	Reference
Polystyrene/divinylbenzene (PS/DVB)	PLRP-S and PRP-1	220	[16]
Graphitized carbon	Hypercarb	225	[18]
Silica, polydentate	C_{18}	100	[19]
Silica, encapsulated	C_{18}	200	[20]
Zirconia supported column	Zirchom PBD, ZichromPS, ZichomCarb	140	[21]
	Diamondbond- C_{18}	180	[22]

A number of studies on the stability and life time of different columns were carried out. Claessens[19] found poor stability for ODS silica materials even when used in

methanol-water eluent, but higher stability for hybrid and polydentate bonded silicas, polymer and zirconia-based materials. Wilson[23] compared Hypercarb, PS-DVB, zirconia-based columns and silica-based columns in the study of pharmaceuticals under superheated water conditions. Hypercarb and PS-DVB columns were stable up to 200 °C. Silica-based columns at 160 °C produced particularly good results, although it was specified that these columns were not stable at this temperature. Shortly afterward, Yang and He[24] found that ZirChrom-PS, PRP-1, Zorbax C8, Nucleosil-C18AB and Hypersil BDS C18 were unaffected after 6000 column volumes at 100 °C. After a series of studies, they concluded that PRP-1 columns were more suitable than others for SHWC.

Silica-based column materials

Separations on silica-based stationary phases are typically performed at room temperature or slightly above, generally up to 70-80 °C. In a number of studies, C18 phases have been used successfully for SHWC, but their lifetimes were short.[23] The problem was caused by the loss of the bonded phase. To provide more stable columns, embedded or hybrid silica-based stationary phases were developed to work at elevated temperatures. For example, polymer-encapsulated silica can be stable at 200 °C, but the stability is limited to 100°C with 100% water or in the presence of organic modifiers.[21] Polydentate bonded C8 stationary phase was used up to 100 °C.[23] Of the hybrid silica phases, Xterra C18 and C8 can be used up to 140 °C, and Xbridge-C18 is useable up to 200 °C.[22]

Zirconia-based column materials

Zirconia, ZrO_2, is much less water soluble than silica. Alkyl-bonded zirconia

stationary phases have great thermal stability (see **Table 1-2**). Although commercially available columns have a recommended limit of 150 °C, Carr et al. suggested that the stability of Zirchrom PBD (polybutadiene) is up to 200 °C in an early study.[25] Later, Wu et al. found a PBD zirconia monolithic capillary column to be stable at 150 °C for over 200 h, but it could be used up to 260 °C.[26] Recently, it was shown that the zirconia phase was stable at 195 °C after 5000 column volumes. The problem with these kinds of materials was that bleeding occurred during temperature gradient and caused repeatability problems, particularly in quantitative measurements.[27] However, zirconia-based stationary phases seem to be on the way to become the most used stationary phases when working at very high temperatures.

Carbon-based materials

Graphitic carbon phases are much more hydrophobic than other existing stationary phases. Consequently, they are subject to contamination problems and produce poor peak shapes and/or low efficiency because of their strong retaining capability. Nevertheless, graphitic carbon materials have high thermal stability and have been successfully used for SHWC.

PS-DVB column materials

Most of the early studies used PLRP-S or PRP-1 columns because of their good resistance to both extreme pH values and temperature changes.[16] They proved to be suitable for SHWC. However, the main problem with this kind of materials is their high retention capacity, similar to graphitic carbon columns. The retention capacity largely depends on the nature of the solutes, and is high even for moderately polar compounds.[24]

Detection in SHWC

The selection of detection methods in conventional liquid chromatography is often limited due to the presence of organic constituents in the eluent. This has led to the dominance of UV/visible and fluorescence methods of detection. RI and electrochemical detection methods play a minor role in gradient separations. More universal methods, such as ELSD, MS and charged aerosol detection, are attractive but have limitations often determined by the volatility of the analyte. As a result, all of these detection methods suffer from certain disadvantages, e.g. time consuming character (e.g. when derivatization is required), poor sensitivity (RI, FT-IR), non-linearity (ELSD), or high cost (MS). The need for a more universal and sensitive detector in HPLC is obvious.

One of the reasons for the interest in using superheated water is that it expands detection selection, simplifies detection methods and improves the sensitivity of most detectors. Because the composition of the mobile phase in SWHC is constant, temperature programming is usually required to separate the analytes. Consequently, the effect of the mobile phase composition change is eliminated, which is of particular importance for MS, ELSD and IR detection. Moreover, because water is transparent to most detectors, new detection modes become possible or the characteristics of existing detection modes can be improved. For example, proton nuclear magnetic resonance (^{1}H-NMR) can be applied for detection by using heavy water as the eluent, UV detectors can work at wavelengths as low as 190 nm, and FID, a universal detector widely used in GC, can be applied in HPLC separations, which is of particular importance. On the other hand, since conventional HPLC detectors work at ambient temperature or slightly higher, the temperature drop of the eluate between the oven and the detector in SHWC may potentially cause solute deposition and/or result in peak broadening. A water bath or an ice bath is usually used to cool the eluent before detection. The operational limits and the

need for cooling are determined by instrumental limitations of the detector used in each case.[14]

FID has a nearly universal response to organic compounds, reasonable sensitivity (LOD of 2 pg/s) and very broad linear dynamic range (10^7).[1] It also offers long-term stability, fast response and simplicity of operation and construction. Since water has no significant FID response, it is possible to use FID as a detector in SWHC. FID is not heat-sensitive, hence the need for post-column mobile phase cooling could be eliminated. The coupling of HPLC and FID is attractive since it can be used to detect non- or poorly UV-absorbing compounds, such as aliphatic alcohols, amino acids and carbohydrates.

In a typical FID, the eluate from the column passes through an air-hydrogen flame. The eluate is burned in the flame. Burning hydrogen in air produces only a trace amount of ions. An increase in ionization occurs when carbon atoms present in the eluate (except carbonyl and carboxyl carbons) generate CH radicals, subsequently producing CHO^+ ions in the flame. Only about 1 in 10^5 carbon atoms produces an ion. The level of ionization is proportional to the number of carbon atoms within the sample. As shown in **Figure 1-5**, an electrostatic field is set up around the burner. The ions generated in the flame carry the electrical current from the anode flame tip to the cathode collector. This electrical current is measured as the detector signal.[1]

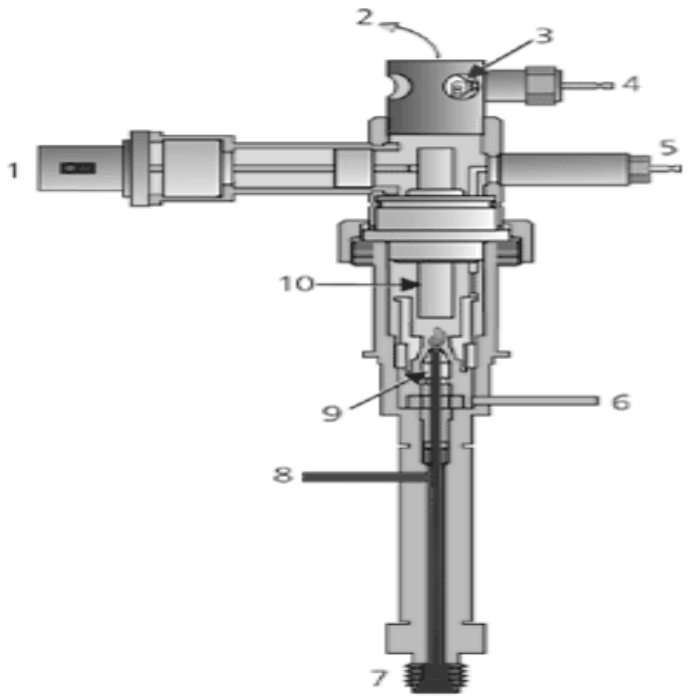

Figure 1-6. Flame ionization detector (FID) cross-section.[28]
1-electrometer connection, 2-effluent exit, 3-ignitor coil, 4-ignitor power connection, 5-polarizing voltage supply connection, 6-air input, 7-column connection, 8-hydrogen input, 9-flame jet, 10-collector electrode.

1.4 Evolution of HPLC-FID Coupling

In the 1980s, the LC-FID prototypes were using a moving belt,[29] wire,[30] chain,[31] or a rotating disc,[32] with the column effluent being applied on the moving substrate and evaporating the mobile phase. All those systems had complex designs and volatile analytes were lost during solvent evaporation. Consequently, FID was replaced with other detectors in HPLC. In the earliest SHWC study, Guillemin et al.[33] presented high temperature water separation of aromatic compounds, carbohydrates and iprodione. An FID was used in their research, but only at an elution temperature of 40 °C.

In 1997, Miller and Hawthorne[34] described the use of subcritical water as a mobile phase for coupling packed-column reversed phase HPLC (RP-HPLC) (15 cm x 2 mm i.d.)

with FID. Limits of detection (LODs; S/N=3) for butanol were 1 ng with water flow between 20 μL/min and 50 μL/min, and 5 ng with flow of 100 μL/min to 200 μL/min, respectively. In their work, the column was connected to the FID with a stainless steel restrictor (57 μm i.d.), and the temperature of the FID was 400 °C. They found that restrictor positioning in the FID was one important factor on flame stability. The best conditions for FID sensitivity and stability were achieved when the restrictor was placed 3 cm below the tip of the FID jet. To maintain the FID flame, gas-flow rates were optimized according to the water flow rate. Hydrogen flow rate played an important role in the stability of the FID response. A large increase in the hydrogen flow rate from 20 mL/min at a water flow rate of 20 μL/min to 300 mL/min at a water flow rate of 200 μL/min was necessary, while a relatively small increase in air flow rate was needed, from 240 mL/min to 430 mL/min, respectively. The importance of restrictor positioning in the FID was further confirmed by Ingelse et al.[35] A capillary restrictor (100 cm x 50 μm) separately thermostated at 300 °C was used to prevent the hot water from sputtering in the restrictor. Stable FID signals were achieved during the detection of alcohols and aldehydes separated at 175 °C. Moreover, Smith et al.[16] reported the determination of parabens in both isothermal and temperature programmed elution, with a similar interface. However, they found problems with restrictor plugging, especially when analyzing nonvolatile analytes such as carbohydrates. The reason for blocking the heated fused silica capillary was analyte deposition and/or degradation, as well as reactions of silica with water at high temperature.

Alternatively, splitting the water effluent (1:10-1:17) before the FID was investigated by Yang et al.[36] The FID was very stable in the split mode even at a total flow rate up to 1.24 mL/min. A stainless steel restrictor (80 cm x 40 μm i.d.) instead of fused silica capillary restrictor was used with the FID, and a fused silica capillary

restrictor (93 cm x 103 μm i.d.) was used on the split line to a waste bottle. The FID temperature was 350 °C and the distance between the restrictor and the tip of the FID jet was 5 cm. However, restrictor plugging occurred as the same problem reported by Ingelse.[35] The linear dynamic range was up to three orders of magnitude, and LODs ranging from 38 ng to 111 ng (306-952 ng/μL injected) were obtained for the separation of several carbohydrates, carboxylic acids and amino acids. In another study, Nakajima et al.[37] determined the ethanol content in alcoholic beverages with a directly coupled HPLC-FID system in a split flow mode. They found the values equivalent to those obtained with a GC-FID measurement. Later, a similar study was proposed by Guillarme et al.[38] They separated lower alkanols on a narrow bore column with water-flow rate ranging from 20 μL/min to 100 μL/min and carried out a detailed optimization of the gas and water flow rates and the FID temperature regardless of the instrument used. In all these studies, the FID temperature and the position of the tip of the restrictor relative to the flame were important for the stability of the FID signal.

As a part of studies on HPLC-FID coupling, Hooijischuur et al.[39] evaluated on-line coupling of micro-column liquid chromatography (μLC) with FID using aqueous eluents. The eluent-jet interface was connected to the FID and generated a jet of droplets by inducing a sharp temperature gradient at the tip of the introduction capillary. It was used for the flow injection analysis (FIA)-FID detection of phenols, carboxylic acids and amino acids in water and for μLC-FID determination of lower alcohols and bis(2-hydroxyethylthio)alkanes at around 10 μl/min.

Recently, Smith and his coworkers[40] used an ambient temperature ICP nebulizer and a spray chamber to generate a mist which carried the analytes to the FID. Column flow rates of 1 ml/min were used in the analysis of carbohydrates, amino acid and

carboxylic acids. Linear responses over a wide range were obtained in each case. However, the sensitivity of the method was poor because of the low analyte transfer efficiency of the nebulizer.

1.5 Optimization and Experimental design

Experimental design is employed in four main areas: screening, optimization, saving time and quantitative modeling. Optimization is one of the most common applications in analytical chemistry. The major goal is to systematically examine different problems that arise within research and development, and to improve the response. This task is usually performed by using one factor at a time method. The main disadvantage of one factor optimization is that there is a risk of misinterpreting results when important interactions between the factors are present. It is also time-consuming. Therefore, an efficient and fast optimization design is essential. The most prevalent are two types of designs: simultaneous and sequential methods (based on objective criteria). Several typical designs for these two categories are briefly described below.[41]

1.5.1 Simultaneous Methods

With simultaneous strategies, the relationship between the response and factors is studied by constructing a mathematical model. The experiments are performed at selected levels of factors. Response surface methods (second-order model) are used to investigate the relationship, and map the optimum region. There are several different types of designs discussed below.

Factorial Design

Factorial design, a first-order model, is performed by varying all factors simultaneously at a fixed number of levels for each factor. A significant advantage of factorial design in comparison with the one-at-a-time approach is the fact that factor interactions can be detected. The most popular design is the two-level full or factional factorial, in which every factor is studied at only two levels. Both of them are often used to detect the influential factors (screening). For two level full factorial designs, 2^k experiments for all possible combinations are required where k is the number of factors. Alternatively, two level fractional factorial designs reduce the number of experiments to 1/2, 1/4 or 1/8 of the total. Two examples of factorial designs are shown in **Figure 1-7,** and all factor combinations are summarized in **Table 1-3.** [41]

Full factorial design (2^k) is very useful in preliminary studies or as an initial step of optimization, while fractional factorial design (2^{k-1}) is mandatory when high factor numbers are involved. However, there are some limitations for factorial designs at two levels: 1) information for replicates (experimental errors) and quadratic terms cannot be accounted for, and 2) only linear predictions are represented. Therefore, the models fit to this type of designs are somewhat restricted.

Table 1-3. Two level full factorial design for three factors, 2^3design. The star labeled experiments represent the half fractional factorial design of **Figure 1-7b** [41]

Experiment	Factors			Response
	x_1	x_2	x_3	
1	-	-	-	y_1
2*	+	-	-	y_2
3	+	+	-	y_3
4*	-	+	-	y_4
5*	-	-	+	y_5
6	+	-	+	y_6
7*	+	+	+	y_7
8	-	+	+	y_8

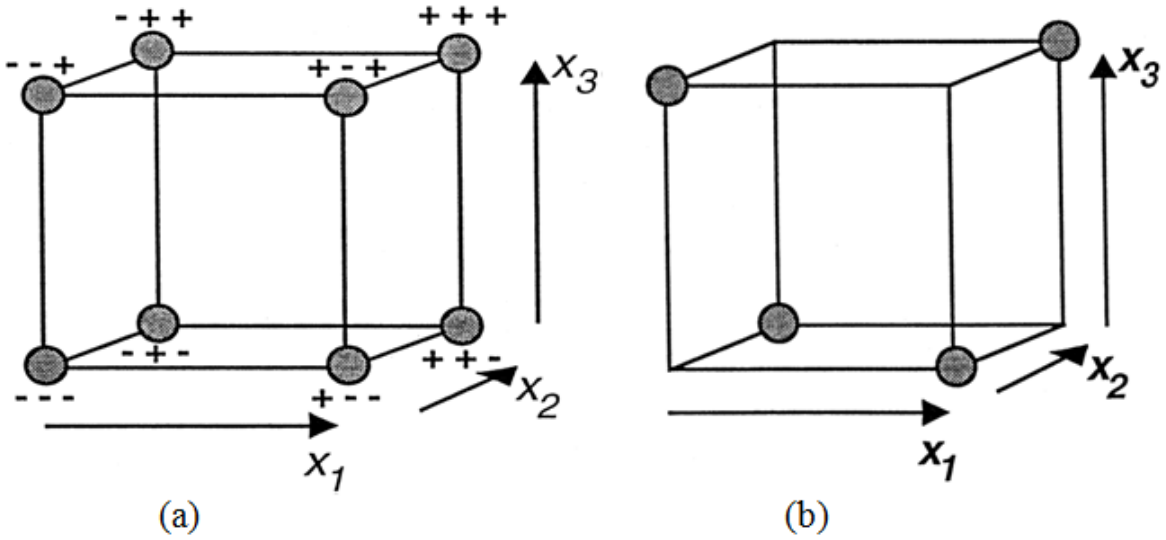

Figure 1-7. Factorial design at two levels. (a) 2^3 full factorial design (b) 2^{3-1} fractional factorial design. x_1, x_2, and x_3 represent the three factors.[41]

Central Composite Design

A central composite design consists of a two-level k-factor factorial design with 2^k factor combinations and an additional star design with 2k+1 factor combinations. If the centers of both designs coincide, they are called central composite designs. The total number of factor combinations is 2^k + 2k +1. This type of designs fits a second-order polynomial, which is very useful as empirical model in many systems over a limited domain of factors. In **Table 1-4,** an example of all factor combinations of a composite

design for three factors is listed. A full factorial design (2^3 experiments) provides estimates of all interaction terms; a star design (6 experiments) is used to estimate the square terms; and typically 5 replicates are used to estimate experimental errors. All factor combinations form a central design with replication.

Table 1-4. Cental composite design for three factors[41]

	x_1	x_2	x_3
2^3 Full factorial	1	1	1
	1	1	-1
	1	-1	1
	1	-1	-1
	-1	1	1
	-1	1	-1
	-1	-1	1
	-1	-1	-1
Star	0	0	-1
	0	0	1
	0	1	0
	0	-1	0
	1	0	0
	-1	0	0
	0	0	0
Replication	0	0	0
	0	0	0
	0	0	0
	0	0	0
	0	0	0

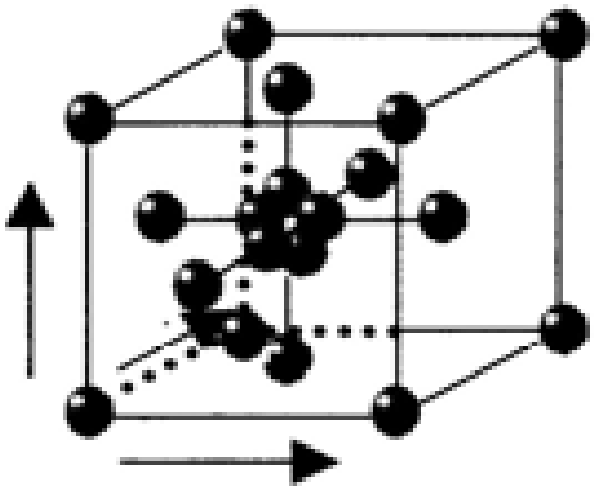

Figure 1-8. Face centered cube composite design for three factors [41]

1.5.2 Sequential methods

With sequential strategies, evaluation of the quantitative relationship between the response and factors is not necessary. Instead, optimization is based on an initial experimental design followed by a sequence of further experiments in the direction to reach the optimum (maximum or minimum) of the response surface. Sequential designs are particularly useful for obtaining guidance at the beginning of a study when only limited knowledge is available about how far the optimum region is from the starting experimental point. The most notable sequential designs include evolutionary optimization design (EVOP) and simplex design. EVOP technique is used mostly in the chemical industry. It requires very large number of experiments in each factorial design (2^k), which is unsuitable for multifactor problems in analytical chemistry. Simplex optimization is a more efficient alternative.

Simplex Optimization

The theoretical basis of simplex optimization was described early by Spendley and co-workers in 1962.[42] Simplex optimization is a valuable, simple and practical approach which has been applied successfully for optimizing multifactor systems in many analytical problems and especially in chromatography.

In principle, a simplex is a multidimensional geometrical object with k+1 vertices, where k is equal to the number of variables in a k-dimensional space: a line in one dimension, a triangle in two dimensions, a tetrahedron in a three-dimensional space, and so forth. Simplex optimization is a stepwise, model-independent strategy. This means that a series of experiments are performed one by one by changing the values of the control parameters (called variables) until a desired quality of response is obtained. First of all, the quantity to be optimized should be determined depending upon the use intended for the final system. An experiment might yield only one response, but more often produces several responses. In this case, the most important one is followed with the simplex series, meanwhile all auxiliary responses are recorded as well. After the optimum on the main response is reached, the additional responses can be used to judge the global optimum.

To construct the initial simplex, the first step is to choose the number of factors of interest (k) and to code these factors to set k+1 experimental starting vertices (corners). For two factors, there are three starting vertices which can be represented as a triangle. The experimental response on each corner of a simplex is ranked, and the corner showing the worst result is reflected through the geometrical midpoint of the other corners. In this way, a new simplex is obtained. The coordinates (experimental settings) for the new corner are calculated. The experiment is performed. After ranking the responses obtained at the corners, the worst of the corners in the new simplex is reflected in the same way as

earlier, and a next new simplex is obtained. In this way, the optimization continues until the simplex starts rotating around the optimum.

Location of the Initial Simplex

To simplify the optimization, the most important factors are chosen by evaluating the change in response caused by a change in the level of each factor. This is based on preliminary experimentation. Also, fractional factorial or Plackett-Burman (P-B) designs can be used to evaluate the significance of all factors involved. Sensible initial conditions and coding of the factors are essential. The initial values of factors are used prior to the investigation, unless preliminary experimentation suggests otherwise. Once the starting point is established, the remaining points are chosen according to the desired step size. **Table 1-5** can be used to construct the starting simplexes of up to seven factors. For the initial location of each vertex (or point), the values in **Table 1-5** specify fractions of the step sizes, which are taken as the distance from the experimental origin (0,0,...,0). The first point with coordinates of (0,0,...,0) is the experimental origin and corresponds to the factor levels used before optimization. For the remaining points, the step size for each factor is multiplied by the corresponding fraction located in **Table 1-5.** Each result is then added to the starting value for each of the factors at the experimental origin (Vertex 1). The new coordinates for each vertex are calculated in the same way. For example, a two factor simplex is a triangle, therefore requires three vertices (1, 2 and 3). The values in **Table 1-5** are used to calculate the set of experimental coordinates needed to establish the initial simplex.

Table 1-5. Initial location of vertices[43]

Vertex	Factor						
No.	A	B	C	D	E	F	G
1	0	0	0	0	0	0	0
2	1.000	0	0	0	0	0	0
3	0.500	0.866	0	0	0	0	0
4	0.500	0.289	0.817	0	0	0	0
5	0.500	0.289	0.204	0.791	0	0	0
6	0.500	0.289	0.204	0.158	0.764	0	0
7	0.500	0.289	0.204	0.158	0.109	0.756	0
8	0.500	0.289	0.204	0.158	0.109	0.094	0.750

Calculation of Simplex Reflection Move

After the first simplex has been run, the response is measured at all vertices, and ranked as 'best', 'next to worst' and 'worst'. The worst response is eliminated and a new vertex is located by reflecting the simplex in the factor space in the direction opposite to the undesirable result.

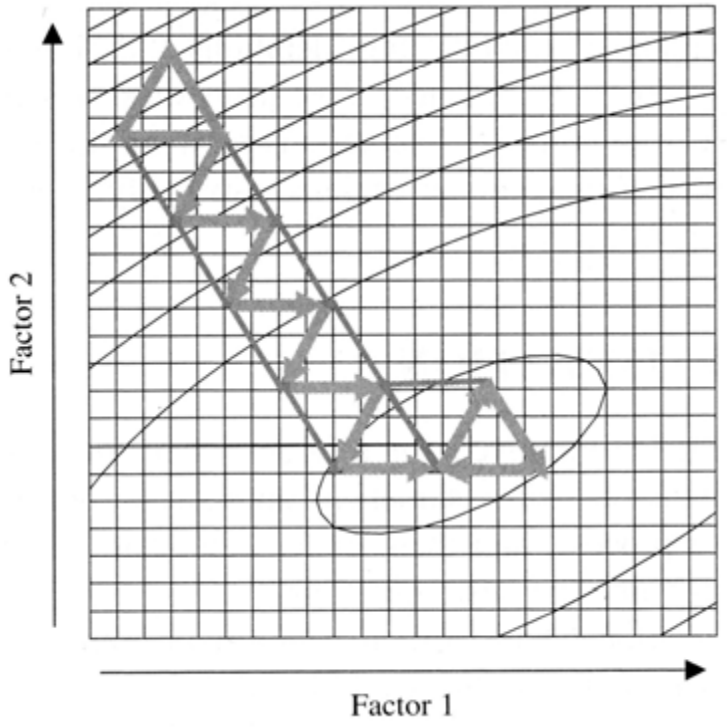

Figure 1-9. Progress of a two factor simplex[41]

In **Figure 1-9**, an example of the process for a two dimensional simplex is presented. The first simplex is the top left triangle. The size of each side of the triangle is called the 'step size'. For a move, the new coordinates for the reflected vertex are calculated using the form in **Table 1-6**. This form also can be used for multifactor simplex, but it is hard to visualize the optimization in n-dimensional space. To obtain the coordinates of the reflected vertex, the coordinates of the retained vertices are first tabulated, and then the sum of each factor is multiplied by 2/k (where k is the number of the retained vertices). Finally, the coordinates of the discarded vertex are subtracted to obtain the coordinates for the new point.

Table 1-6. Table for Simplex Reflection[43]

	Vertex No.	Factor			
		A	B	C	D
k retained vertices	1 2 3 4 .				
Sum of retained coordinates……..	.				
2/k * (sum)……..	.				
Coordinates of discarded vertex….	.				
Coordinates of new vertex……..	.				

To ensure that moves are made in the correct direction and that the simplex does not get stuck, simplex progression is based on the following rules: 1) after each observation of the response, a move is to be done by carrying out only one additional measurement; 2) the next simplex is obtained by discarding the vertex with the worst response and replacing it with the reflected vertex; 3) if the reflected vertex has the worst response in the new simplex, the second lowest response in the simplex is rejected and the procedure is continued; 4) if the new vertex lies outside the physical constraints of the variables, the vertex is regarded as the lowest-achieving. Rules 1-4 are employed to force

the simplex back to its boundaries. The final rule (5) is that once the simplex starts to rotate around a vertex, the size of the simplex is reduced to find the optimum more accurately.

The rules of regression and calculation of reflection described above are used for construction of a fixed-size simplex design. The fixed size might lead to problems when improper step size is chosen. If it is too large, a step might overshoot the optimum; if it is too small, the number of experiments required becomes very large, and errors might be greater than the changes in response. These disadvantages can be avoided by using the variable-size simplex, which allows finding the optimum faster and more accurately.

Variable-Size Simplex

With the variable-size simplex, the step size is changed by expansion or contraction of the reflected vertices (see **Figure 1-10**). The algorithm is modified as follow:

R = P+(P-W) (the first reflection)

1) If the response at R is better than B, the simplex is expanded.

E = P+2(P-W)

a) If the response at E is better than at B, the new simplex BNE is retained. If it is worse than

at B, the simplex BNR is retained.

b) If the response at R is between that at B and N, the new simplex is BNR.

2) If the response at R is worse than at B, the simplex is contracted according to :

a) The response at R is worse than at N, but better than at W, the new simplex is BNC_r.

C_r = P+1/2(P-W)

b) The response at R is worse than at W, the new simplex is BNC_w

C_w =P-1/2(P-W)

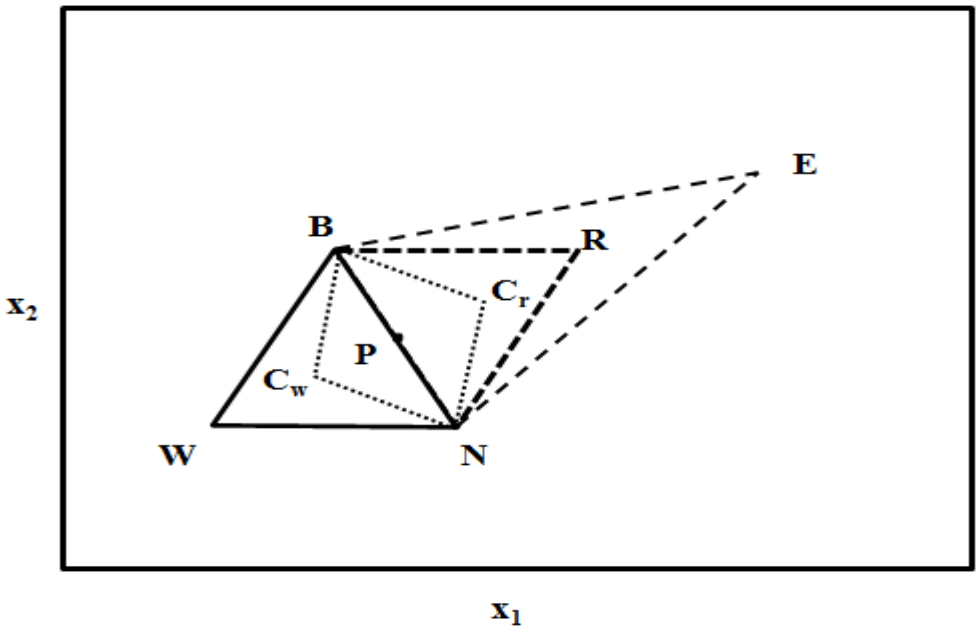

Figure 1-10. Variable size simplex algorithm - summary of moves[41]

1.6 Objective

Due to the relatively large volume of the mobile phase in HPLC, flame-based selective detection systems face problems with flame stability. In SHWC, attempts were made to reduce the amount of water introduced into the FID. The experimental HPLC-FID coupling was carried out in the split or splitless mode. Most of the approaches utilizing the splitless mode were based on an interface, leading either to eluent evaporation or to formation of a stream of small droplets at the outlet of the column. In this project, HPLC-FID coupling using pure water as the mobile phase was explored, and universal detection by HPLC-FID was examined.

Chapter 2.0 - Optimization of the FIA-FID Coupling

2.1 Introduction

The basic idea of this project was to deliver the column eluate directly to the FID flame in the form of a liquid filament generated at the outlet of a suitable small I.D. restrictor, thus bypassing the need for eluate evaporation inside the FID jet at high temperature, which usually results in numerous problems. The critical issue in this project was how much water could be vaporized in the time the aqueous eluate needed to pass through the flame, since all the water should be vaporized before the analytes could be detected. Increasing the rate of evaporation of the effluent was the main goal of this project. First of all, the preliminary experiments were carried out in the GC mode in order to establish the baseline reference for detector sensitivity and linearity for future studies involving HPLC-FID coupling. Secondly, a liquid filament of the effluent from the outlet of the injection valve was directed towards the flame of the FID via a restrictor in flow injection mode. A column was not used. In this case, a series of improvements were tested in order to reduce the amount of water passing through the flame of the FID for FID stability tests. Optimization of FID parameters was carried out using two different setups of the FID (see **Figure 2-1**).

Non-volatile compounds such as carbohydrates and pharmaceutical compounds were primarily analyzed in this project. As the starting point, glucose was used as the target compound.

2.2 Experimental Section

2.2.1 Chemicals and Materials

C8-C13 n-alkanes and glucose used in preliminary experiments were purchased from Sigma-Aldrich (ON. Canada). Hydrogen, compressed air, nitrogen and oxygen gas cylinders were purchased from Praxair Canada Incorporated (Ontario, Canada). Palladium wires (0.5 mm and 0.1 mm I.D.) were purchased from Alfa Aesar (A John Matthey Company, MA. USA). A modified FID jet was made in-house by the machine shop at the University of Waterloo. Throughout the study, deionised water (Milli Q water purification system; Millipore, Milford, MA, USA) was used.

Preparation of Liquid Standards

A preliminary study involving determination of the calibration curves and detection limits in GC mode was carried out using a mixture of C8-C13 n-alkanes. Preparation of liquid C8-C13 n-alkane standards ranging from 2.5 ppm to 500 ppm was performed through the following procedure: a stock solution including 1 mg/mL each of octane, nonane, decane, undecane, dodecane and tridecane in carbon disulfide was used. The standard solutions were prepared by dilution of an aliquot of the stock solution with carbon disulfide in a 100 mL and/or 50 mL volumetric flask. The characteristics of the standard solutions prepared by dilution are summarized in **Table 2-1**.

A solution of ~0.5% glucose in deionised water was prepared for optimization of the FID parameters. A weight of 0.766 g glucose powder was dissolved in deionised water in a 10 mL beaker. The solution was filtered and transferred into a 100 mL volumetric flask. Deionised water was then added to the mark, and the solution was well mixed. The solution in the volumetric flask was degassed in a Model 275D Crest

Ultrasonic cleaner (Crest Ultrasonics Corp. NJ. USA) for 30 minutes at a temperature of 35 °C.

Table 2-1. n-Alkane Standard Series Prepared by Dilution

	C8	**C9**	**C10**	**C11**	**C12**	**C13**
Stock target (1000 ppm) 10 mg/10 mL	10	10	10	10	10	10
Density (g/mL)	0.703	0.722	0.730	0.740	0.753	0.756
Volume required for 10 mg	14	14	14	14	13	13
Actual weight weighed into 10 mL	9.3	10.1	10.6	11	9.1	10.1
Concentration (µg/mL)	930	1010	1060	1100	910	1010
Dilution 1 (2.5 mL stock in 5 mL)	465	505	530	550	455	505
Dilution 2 (1 ml stock in 10 mL)	93	101	106	110	91	101
Dilution 3 (1 mL diln 2 in 10 mL)	9.3	10.1	10.6	11	9.1	10.1
Dilution 4 (2.5 mL diln 3 in 5 mL)	4.65	5.05	5.30	5.50	4.55	5.05
Dilution 5 (1.25 mL diln 3 in 5 mL)	2.33	2.53	2.65	2.75	2.28	2.53

2.2.2 Instrumentation

Preliminary Work

An SRI instrument Model 8610C GC/FID equipped with two FID detectors was used in the project. Preliminary experiments were carried out in the GC mode. The GC was equipped with a split/splitless injector. One microliter manual injections were carried out using the hot needle technique. A narrow neck liner (i.d. 0.8 mm) was placed inside of the heated injector, which was connected to an MYF 1301 GC capillary column (15 m x

0.28 mm i.d.). The injector temperature was maintained at 250 °C. All results were obtained using a temperature program which started at 60 °C for 1 min, and then ramped at 30 °C/min to 250 °C. Nitrogen was used as the carrier gas at a constant flow rate of 6 mL/min. FID gas flows (hydrogen and air) were 25 mL/min and 250 mL/min, respectively, as recommended by the manufacturer of the instrumentation. The needle was held in the hot injector for approximately 4 s, and then the sample was injected quickly by hand.

Two different setups of the FID were tested: cathode positioned directly opposite the flame, and placed perpendicularly to the jet (see **Figure 2-1**). A mixture of C8-C13 n-alkane standards were used in the test.

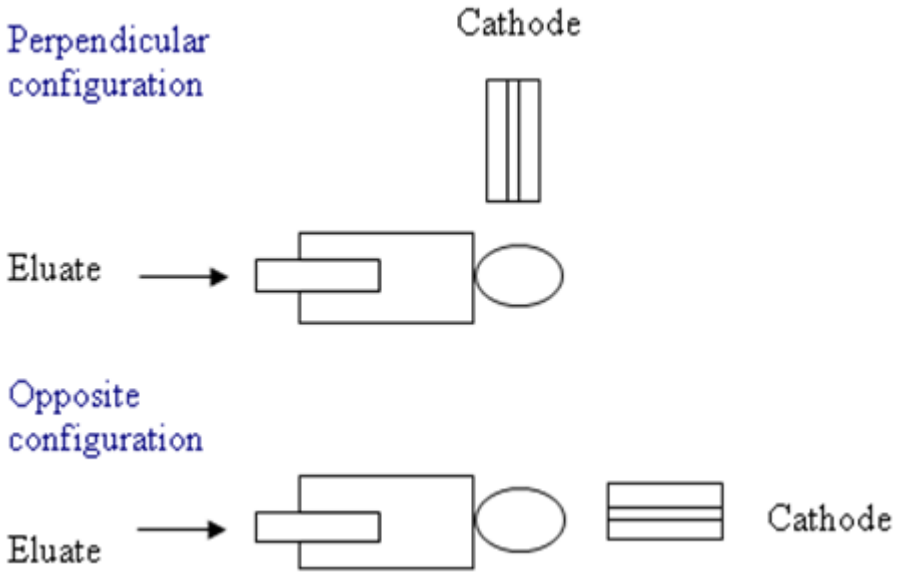

Figure 2-1. Two different setups of the FID

FIA-FID Setup

The online FIA-FID setup is shown schematically in **Figure 2-2**. A TSK-6010 pump (HPLC instruments, USA) was used to deliver the aqueous mobile phase, and was connected to a Rheodyne 7725i manual injection valve with an external 20 µL sample loop (Chromatographic Specialties Inc., ON, Canada) using stainless steel tubing (50 cm x 0.4 mm I.D., Agilent Technologies, USA). The outlet of the injection valve was connected to another piece of stainless steel tubing, which was connected to a fused silica capillary tube (4 cm x 51 µm I.D., 301 µm O.D.) The liquid filament of the aqueous eluate from the restrictor (the fused silica capillary tubing) was directed towards the flame of the FID, on which two different configurations shown in **Figure 2-1** were examined. Experiments were carried out in the flow injection (FIA) mode.

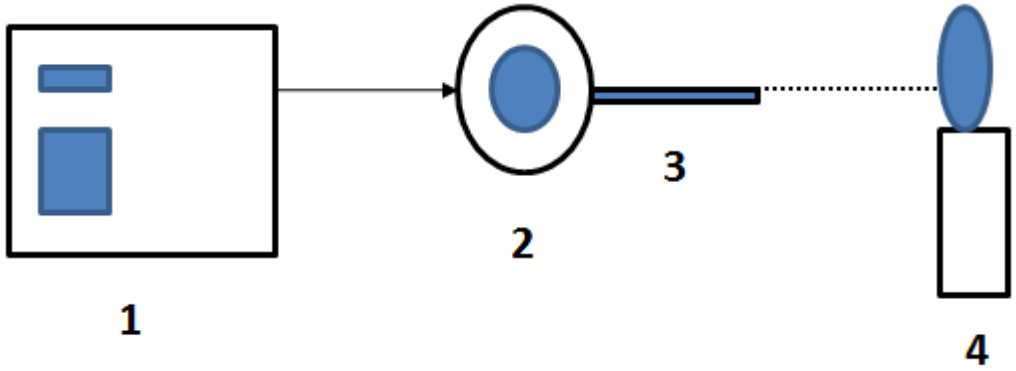

Figure 2-2. Schematic diagram of the FIA-FID setup: 1 - LC Pump, 2 - Injection Valve, 3 - Capillary Tubing (Restrictor), 4 - FID.

Because only the FID detector was evaluated in this study, other parameters involving oven temperature were set to constant values. The details of the instrumental settings are shown in **Table 2-2**. FID data collection and processing were performed using Peak Simple Chromatography Data System software (SRI instruments) ran on a personal computer connected to the GC.

Table 2-2: Instrumental settings for the FIA-FID experiments

Initial oven temperature	60°C
Final oven temperature	60°C
FID temperature	150°C (as the starting point)
Data sampling rate	5 Hz
Integration	Peak 95%
	Baseline 60%

2.3 Results and Discussion

Preliminary results

In the preliminary experiments, a mixture of C8-C13 n-alkanes was used in the tests. Calibration graphs were constructed at 5 concentration levels in the range from 2.5 ppm to 500 pm. Six independent determinations were performed at each concentration. Linear relationships were obtained between the peak area of each compound and analyte concentration. Based on the data provided in **Table 2-3**, calibration curves of peak area vs. concentration for two different cathode configurations were prepared, and are shown in **Figure 2-3**. No significant differences in sensitivity were observed for the two different cathode configurations.

Table 2-3. Peak area vs. concentration for the two FID cathode configurations (based on three replicates)

Perpendicular Configuration											
C8		C9		C10		C11		C12		C13	
Conc. (µg/mL)	Peak Area	Conc. (µg/mL)	Peak Area	Conc. (µg/mL)	Peak Area	Conc. (µg/mL)	Peak Area	Conc. (µg/mL)	Peak Area	Conc. (µg/mL)	Peak Area
465	4208.13	505	6015.46	530	6834.26	550	7333.74	455	7393.71	505	8376.57
93	821.35	101	1252.98	106	1485.23	110	1647.23	91	1640.65	101	1787.16
9.3	55.86	10.1	88.67	10.6	103.99	11	111.50	9.1	116.47	10.1	126.16
4.65	28.18	5.05	45.12	5.3	51.80	5.5	58.10	4.55	56.90	5.05	68.62
2.33	15.22	2.53	26.31	2.65	30.58	2.75	33.63	2.28	35.11	2.53	45.05
Opposite configuration											
C8		C9		C10		C11		C12		C13	
Conc. (µg/mL)	Peak Area	Conc. (µg/mL)	Peak Area	Conc. (µg/mL)	Peak Area	Conc. (µg/mL)	Peak Area	Conc. (µg/mL)	Peak Area	Conc. (µg/mL)	Peak Area
465	4547.02	505	6504.19	530	7570.38	550	7986.43	455	7839.55	505	8419.41
93	758.14	101	1028.23	106	1181.11	110	1259.78	91	1229.51	101	1349.71
9.3	62.14	10.1	85.75	10.6	98.94	11	103.84	9.1	105.19	10.1	125.60
4.65	22.36	5.05	35.84	5.3	40.09	5.5	40.22	4.55	41.21	5.05	45.79
2.33	12.32	2.53	19.60	2.65	22.77	2.75	24.71	2.28	26.60	2.53	30.34

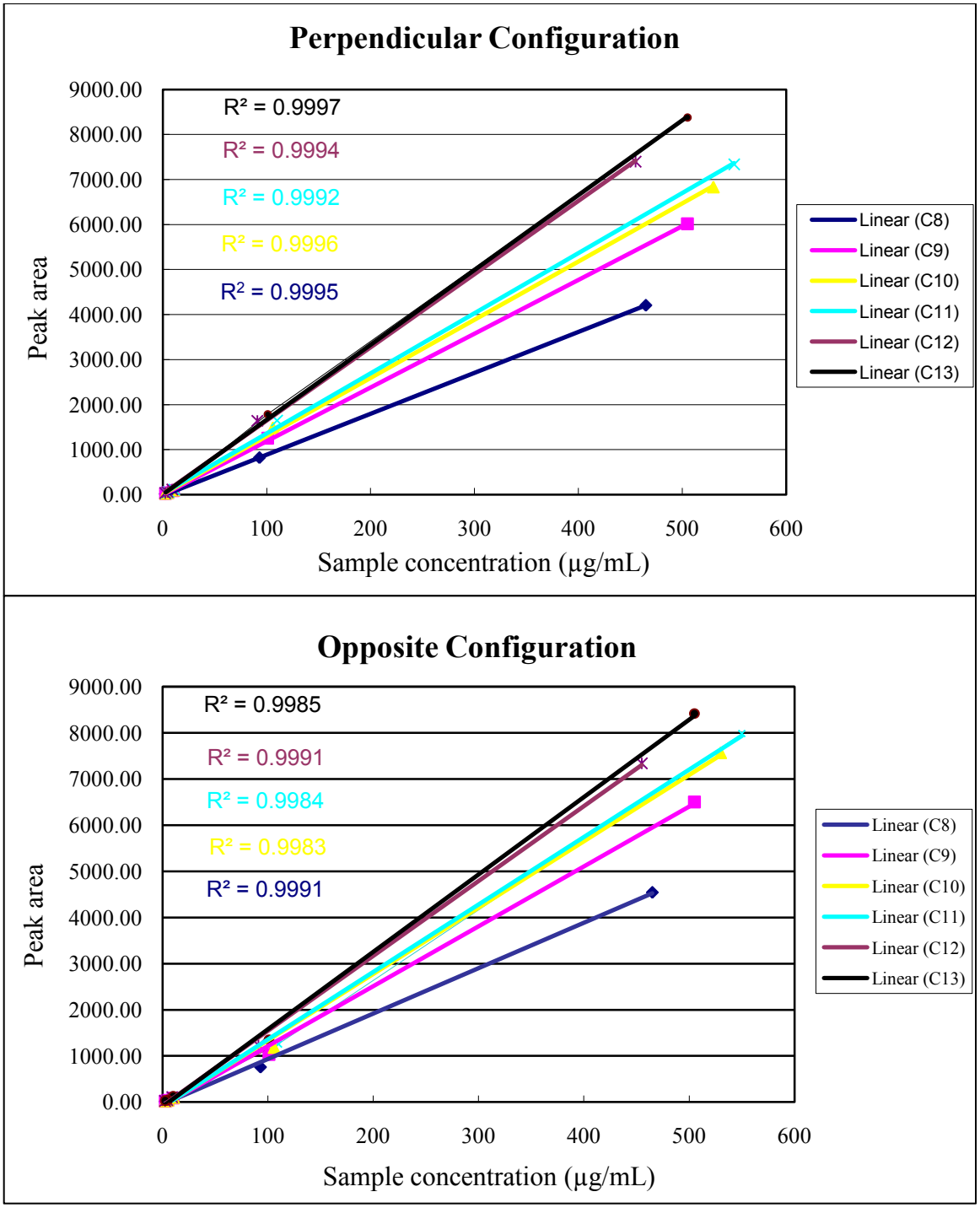

Figure 2-3. Calibration curves for two different cathode configurations: perpendicular configuration on top and opposite configuration at the bottom.

The Influence of water flow rate

To test new ideas, it was necessary to choose an analytical instrument that performed a fast and accurate analysis, and provided the flexibility of easily combining

with other accessories and detectors. Therefore, an SRI instrument Model 8610C field GC/FID was selected for the whole project.

In previous studies, it was shown by different authors that the stability of the FID response depended strongly on the water flow rate when the restrictor capillary was inserted into the FID jet in split or splitless mode. A high water flow rate (greater than 0.15 mL/min) resulted in instability of the FID flame. It was necessary to use a low water flow rate, which resulted in restrictor plugging at high temperatures. In this project, delivering the liquid filament generated at the outlet of a restrictor into the flame of the FID should eliminate problems with restrictor plugging. Water flow rate was still considered a significant parameter.

In order to generate a liquid filament at the outlet of the restrictor, a range of water flow rates from 0.3 to 1 mL/min was tested with different small I.D. capillaries. A capillary tube (4 cm x 50 μm i.d., 301 μm o.d.) was predominantly used as the restrictor in this study. The lowest water flow rate able to generate a liquid filament was 0.55 mL/min. Liquid sprays were observed along and at the end of the liquid filament. With increasing water flow rate, the region of liquid filament without the sprays between the outlet of the restrictor and the spray end of the liquid filament became longer, which was important in this study because sprays along the liquid filament resulted in loss of the analytes, a baseline featuring a high number of spikes, and even FID flameout. On the other hand, a high water flow rate (larger than 1 mL/min) resulted in incomplete evaporation of the aqueous phase and high backpressure, and often no analyte responses were detected. Therefore, a series of experiments was conducted to find the optimal water flow rate relative to the optimal FID conditions in the effective range of water flow rate from 0.55 to 1 mL/min.

The Effect of the Two Different FID Setups

Initially, optimization of the FID parameters and water flow rate was carried out in the flow injection mode using the two different FID setups (see **Figure 2-1**). The column was not used. The details of the instrumental settings including FID gas flows and FID temperature recommended by the manufacturer of the instrumentation were shown in Table 2-2. In the opposite configuration, Milli Q water was used first to test the baseline stability. However, delivering pure water to the flame in the opposite direction with flow rates in the effective range from 0.55 to 1 mL/min resulted in FID flameout. The approach in this configuration was, subsequently, discontinued.

In the perpendicular configuration, the effluent was delivered to the flame from the top end of the FID body, while the residual waste fraction leaving through the bottom end of the FID body was collected in a waste vial. However, FID flameouts were still encountered. As shown in **Figure 2-4**, since more than half of the space inside the detector body was occupied by the tip of the FID jet, the liquid filament could potentially hit the jet directly when the alignment was not perfect. To overcome this problem, a small portion of the FID jet inside of the chamber was machined away in order to avoid blocking the pathway of the effluent delivered through the chamber. A series of experiments were carried out to find the optimal FID conditions in this configuration.

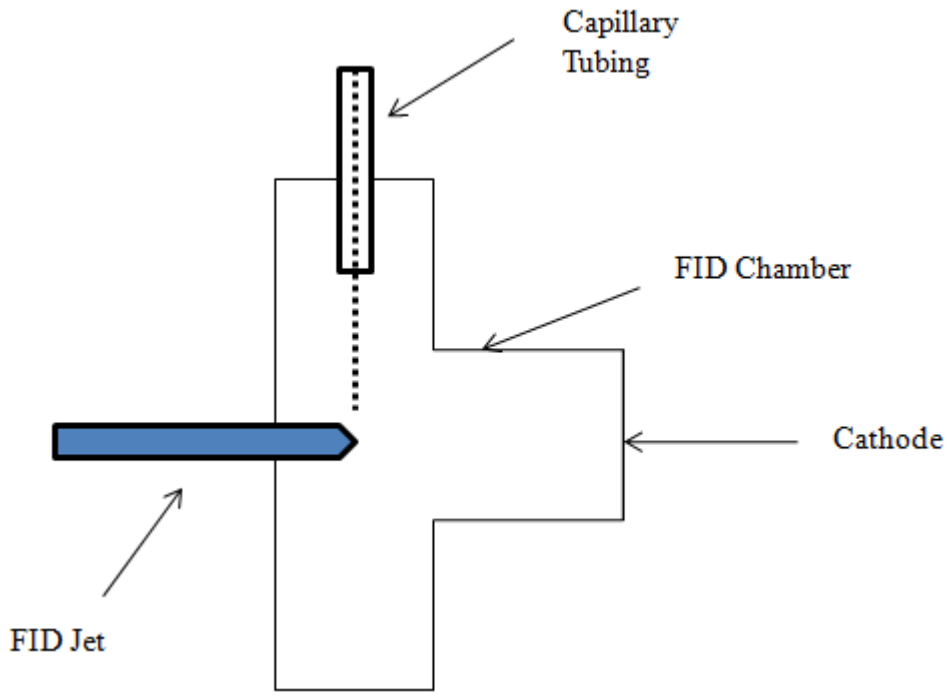

Figure 2-4. The position of the FID jet inside of the FID chamber

FID Optimization in the Opposite Configuration

FID Optimization was carried out in FIA-FID mode. Again, the column was not used. The water flow rate was adjusted to 0.65 ml/min since lower flow rates resulted in baseline instability. A solution of 0.5% (v:v) glucose in deionised water was injected as the sample solution. Its peak areas were used for the evaluation of the FID parameters. The initial FID settings were the following: hydrogen and air flow rates were set at 25 mL/min and 250 mL/min, respectively; FID temperature was set at 150 °C (recommended by the manufacturer). The influence of FID temperature was investigated in the range from 150 °C to 375 °C (maximum setting). At lower temperatures (from 150 °C to 250 °C), FID flameouts were frequently encountered. With increasing temperature, the FID signals became more stable, and larger peak areas of glucose were observed. Therefore, FID temperature was set at 375 °C for the whole project.

The effect of gas flows (hydrogen and air or oxygen) on FID performance was evaluated using one factor at a time method. Hydrogen flow rate started at 30 mL/min, increasing in the interval of 5 mL/min for each run, while air flow rate was set based on hydrogen-air ratio of 1:10. The largest peak area of glucose was observed when the hydrogen and air flow rates were 35 mL/min and 350 mL/min, respectively. It was well known that hydrogen flow rate had the primary effect on FID stability in comparison to air flow rate. In order to evaluate the influence of hydrogen flow rate, air flow rate was set at a constant value of 250 mL/min. Hydrogen flow rate was tested in the range from 25 to 150 mL/min. The best performance was obtained when the hydrogen flow rate was set at 115 mL/min. Due to incomplete vaporization of the effluent in the FID, water droplets from the liquid filament of effluent could hit anywhere inside of the FID chamber, resulting in FID instability and/or band broadening. FID remained lit for a short time. To overcome these problems, two improvements were tested. Premixing hydrogen and air was carried out by placing air delivery capillary tubing inside of the FID jet. In the original FID system, the air input was set beside the FID jet. Compressed air was delivered into the inside of the FID chamber, whereas hydrogen flow was coming out from the tip of the FID jet. An FID ignitor is normally connected to the bottom end of the FID chamber. In this study, the FID ignitor had to be removed to leave the bottom end of the FID chamber open due to incomplete evaporation of the effluent. This setup resulted in incomplete hydrogen-air mixing. Therefore, premixing hydrogen and air improved the quality of flame, and made a hotter and sharper flame. Alternatively, using a palladium wire (0.5 mm or 0.1 mm I.D.) was tested to prevent FID flameouts by putting it into the flame via the jet. Palladium absorbs hydrogen and catalyzes its oxidation in air at room temperature, which was thought sufficient to sustain the flame. Before the use of the

palladium wire, its surface was cleaned by heating with a propane flame. However, FID responses were still not stable. FID flameout was still encountered after a short time.

For further studies, oxygen was tested as a replacement for air to achieve higher FID flame temperature, thus increasing the efficiency of water evaporation. The influence of hydrogen and oxygen flow rates were tested using the same method as studied for optimization of hydrogen and air flow rates. The relative flow rates of hydrogen and oxygen were set at the ratio of 1:2 since air contains about 20.95 % oxygen in total volume. The initial experiment started with a hydrogen flow rate of 25 mL/min, an oxygen flow rate of 50 mL/min. Unfortunately, FID flameout was frequently encountered with an increase of gas flows. Also, irregular shapes of analyte peaks were observed (see **Figure 2-5**).

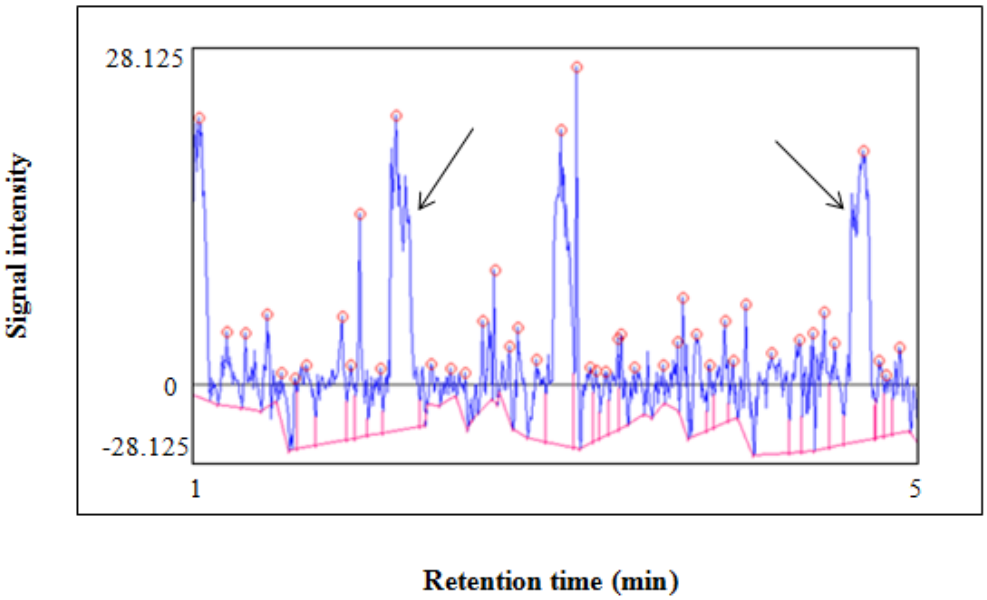

Figure 2-5. The shapes of analyte peaks The arrows indicate the analyte peaks

2.4 Conclusions

The GC method was used first to study the FID sensitivity and linearity in two different FID setups in order to compare with FID conditions in future studies involving

HPLC-FID coupling. The basic idea was to deliver all effluent directly into the FID flame in FIA-FID mode. Due to incomplete vaporization of the aqueous phase, a series of improvements were tested to reduce the amount of effluent passing through the FID flame. Optimization of FID parameters including water flow rate, FID temperature and gas flow rates in two different FID setups was investigated. The optimal FID temperature and water flow rates were 375 °C and 0.65 ml/min, respectively, for all the experiments. In the perpendicular configuration, the best performance was obtained when the hydrogen and air flow rates were set at 115 and 250 mL/min, respectively.

Chapter 3 Optimization of a Modified FID System (I)

3.1 Introduction

Introduction of a liquid filament directly into the flame of the FID resulted in numerous problems when using an unmodified FID detector in the previous section. The biggest problem was FID flameout. To overcome this problem, a modified FID detector was made by the UW machine shop and used. An FID ignitor could be set beside the FID jet to prevent the flameout. In addition, a tubular oven was used before the FID to preheat the effluent and partially evaporate the aqueous mobile phase. All the improvements were tested by using the modified FID detector. The methods and other system settings were the same as used in the previous section. Experiments were also carried out in FIA-FID mode without a column. FID conditions were optimized by using a standard series of glucose solutions.

3.2 Experimental Section

3.2.1 Chemicals and Materials

HPLC grade ethanol and isopropanol (IPA) were purchased from EMD Chemicals, (NJ,USA). Glucose and Milli Q water were used as in the previous experiments. A tubular oven, a part of a dry electrolytic conductivity detector made by SRI, was used. A modified FID jet was made in-house by the machine shop at the University of Waterloo.

Preparation of liquid standards

A solution of 10 % (v/v) glucose dissolved in deionised water was used as a stock standard, which was 15.453 g glucose powder dissolved in 100 mL deionised water. A series of standard solutions were prepared by dilution of aliquots of the stock solution with aliquots of deionised water in 100 mL volumetric flasks by using a volume transfer

burette. The lower concentration standards were prepared by further diluting the intermediate standard through the same procedure. For example, 0.5 % (v/v) glucose solution was prepared by adding 20 ml of 2.5 % (v/v) glucose solution to a volumetric flask, and diluting it with 80 mL deionised water. The standard solution series containing 0.5 %, 1 %, 2.5 %, 5 % and 10 % (v/v) glucose was made and stored at room temperature for future use.

HPLC grade isopropanol was also used in this study. The standard solutions containing 0.1 %, 0.5 % and 1 % (v/v) IPA were prepared using the same procedure.

3.2.2 Instrumentation

The basic components of the system used were the same as those in the previous section, except that the modified FID detector was used. The modified FID was made by centering and soldering a tapered end of stainless steel tubing into a ¼ inch cross union. Subsequently, a miniature high-temperature tubular oven was placed between the modified FID and the outlet of the injection valve in order to reduce the amount of water passing through the flame of the FID. As shown in **Figure 3-1**, the top end of the FID chamber was either connected to the collector electrode (cathode) or to the miniature oven. The GC ignitor was introduced to the FID chamber from the side or from the bottom. The remaining open end of the FID chamber was used for collecting the effluent waste. The FID gas flows (hydrogen and air) were controlled by the GC.

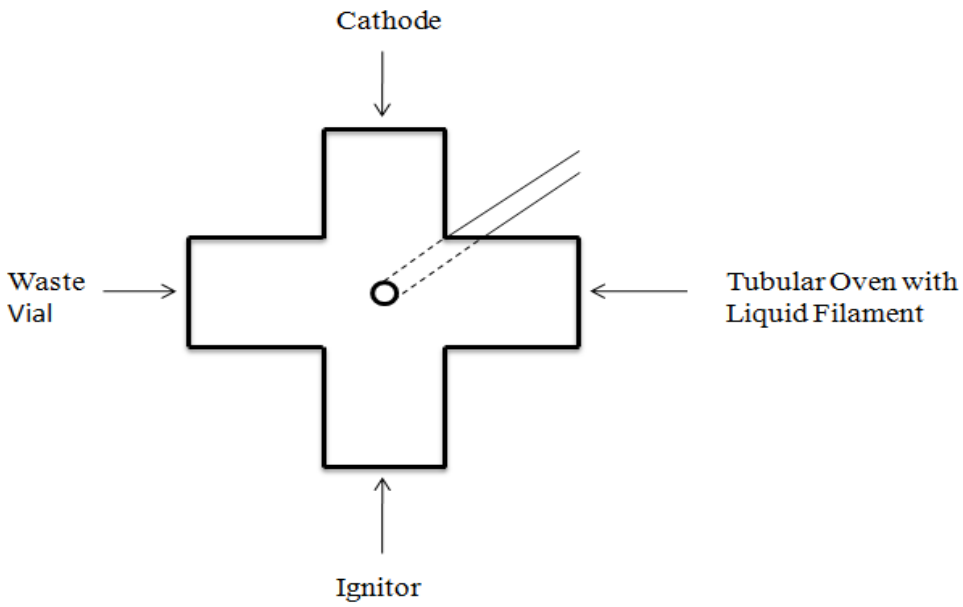

Configuration A

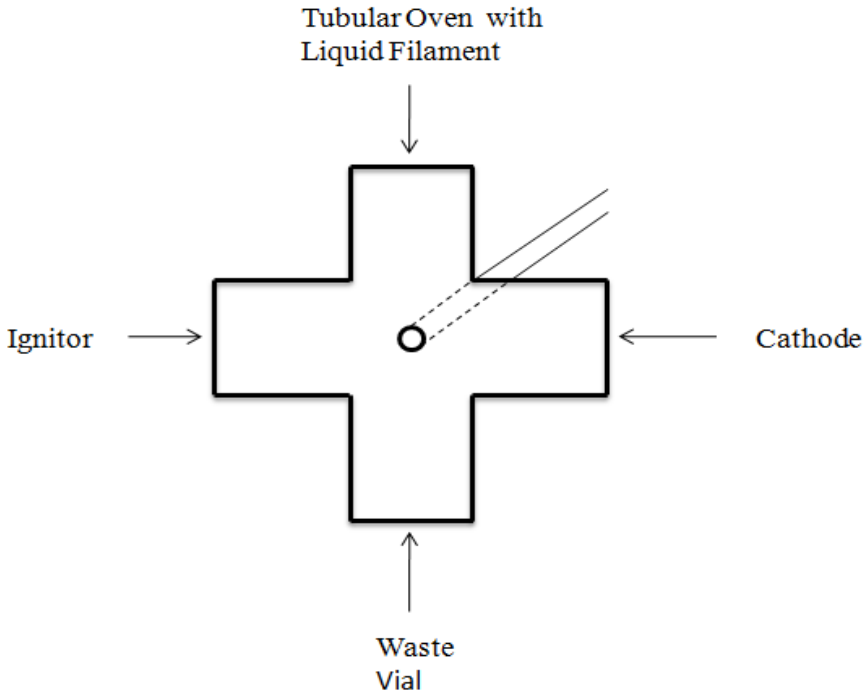

Configuration B

Figure 3-1. The FID configurations used in the study

The Tubular Oven System

A miniature high-temperature tubular oven, originally a part of a dry electrolytic conductivity detector (DELCD) made by SRI, was used in the experiments. Its resistance was 1 ohm. In order to limit the temperature up to about 400 °C, a resistor (output: 6.3V, 4A) was connected in series with the tubular oven, followed by an autotransformer whose input was 120V and output was 0-140V. The temperature inside the tubular oven was measured by using K type thermocouples linked to a multimeter. The oven system is schematically shown in **Figure 3-2.**

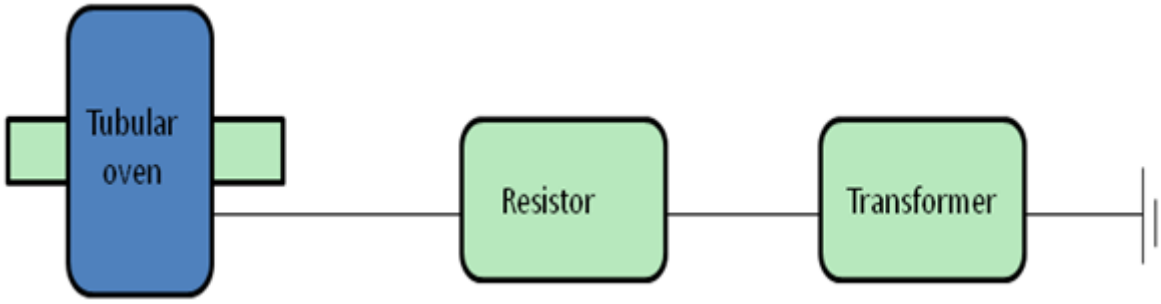

Figure 3-2. The tubular oven system

3.3 Results and Discussion

In the previous section, the best performance of the FID was obtained when the hydrogen and air flow rates were set at 100 mL/min and 250 mL/min, respectively. As shown in **Figure 3-1**, initial experiments were carried out in configuration A and started with the same values of gas flows as above. The temperature of the tubular oven was set at ~235 °C by adjusting the autotransformer to scale reading of 40. The water flow rate was still set at 0.65 mL/min. The FID response did not differ significantly when using the two FID detector configurations. Optimization of hydrogen and oxygen flows was continued in the current setup. The initial hydrogen and oxygen flow rates were set at 10

mL/min and 20 mL/min, followed by increasing both gas flows in the ratio of 1:2 for further study. However, no signals were observed, and the baseline remained very noisy.

Because a hydrogen-air flame cannot be observed by the naked eye, it is hard to estimate acceptable initial gas flows under unstable flame condition. To visualize the intensity of the flame, a simple solution was to check the flame condition by delivering propane gas into the flame. Propane was controlled by a micro regulator and flowed into the FID jet via a T union which was linked to the hydrogen gas line at the other end by using different lengths of capillary tubing. In order to generate enough heat under the stable flame condition, a 4-5 mm length of flame is expected since a large flame can produce more energy. Different hydrogen and oxygen flow rates in the ratio of 1:2 were tested. With increasing gas flows, the color of the flame turned from blue to bright blue. Because the distance between the tip of the FID and the inside wall was less than 4 mm, the shape of the flame was limited by the inside wall of the FID chamber. The initial gas flows were set based on the color change of flame. A hydrogen flow rate of 30 mL/min and oxygen flow rate of 60 mL/min were considered as the initial setting. Gas flows were optimized in two different FID setups, configurations A and B. A standard series consisting of 0.5 %, 1 %, 2.5 % and 5 % (v/v) glucose solutions were injected at a time interval of 1 min three times during each run. However, no analyte signals were observed.

A solution of 0.5 mL HPLC grade ethanol in 2 mL deionised water was used instead of glucose solution to test the reasons for the lack of response. Good FID responses were observed for the above initial settings. Because ethanol has a low boiling point (78 °C), HPLC grade isopropanol (IPA) was also used. Solutions of 0.1 %, 0.5 % and 1 % (v/v) IPA in deionised water were prepared and injected for each run. Optimization of gas flows was carried out for two different FID setups. Other settings such as water flow rate and FID temperature remained the same as used in the previous

experiments. A tubular oven was set before the FID. It was first intended for the liquid filament of the effluent to be delivered to the flame through the tubular oven. It preheated the effluent and partially evaporated the aqueous mobile phase. Nitrogen gas flowing counter currently through the oven was used to remove the water vapour generated in the tubular oven. However, increasing nitrogen flow resulted in flame instability. The use of relatively low N_2 flow rate was necessary, but at the same time, at low flow rates the removal of water hitting the inside walls of the oven was not efficient enough. In addition, the effluent did not evaporate completely in the flame, and excess water accumulated in the FID body resulting in FID flameout. Therefore, in the next attempt, the tubular oven was used to preheat the effluent by feeding the restrictor capillary through it. In addition, two different FID setups were tested (see **Figure 3-1**). The best results were obtained in Configuration B, when the hydrogen and oxygen flow rates were set at 120 mL/min and 115 mL/min, respectively. Still, the detection limit was a disappointing ~0.5 % IPA in solution. Also, irregular shape of analyte peaks was observed. The FID signals were not observed occasionally during the experiments, even under the same condition. Most likely this was due to the position change of the outlet of the capillary.

The Influence of the Position of the Capillary

To overcome this problem, the capillary tubing fed through the cathode was centered and set just above the tip of the FID jet. The position of the capillary is shown in **Figure 3-3**. Optimization of hydrogen and oxygen flow rates was also carried out in the two different FID configurations. Water flow rates ranging from 0.65 mL/min to 1 mL/min were tested. The best performance was observed, when the water flow rate was set at 0.7 mL/min. Hydrogen and oxygen flow rates were tested by an increase in the ratio of 1:2 during the initial stage of the analysis, and then further studied in the ratio of 1:1. The

optimal hydrogen and oxygen flow rates were 130 mL/min and 115 mL/min, respectively. FID temperature was still set at the maximum value of 375 °C.

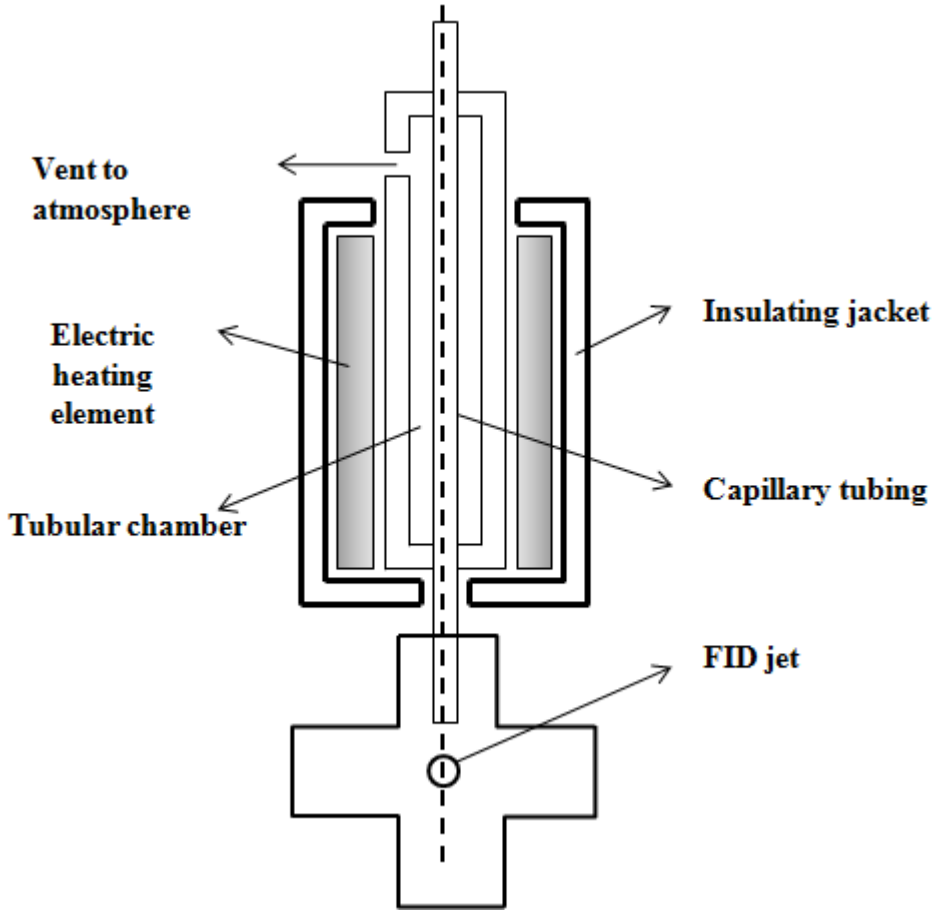

Figure 3-3. The position of the capillary inside the FID chamber

In this project, glucose was considered as the target compound. Hence, the same settings were used in the further study, but glucose solutions were used as a replacement for IPA solutions. During the experiments, popping sounds inside of the FID body were heard, while flash flames in the FID chamber were observed after running for about 2 hours resulting in random spikes of the signal. The problem could be related to any part of the system, including poor cathode connection; leakage problem with the pump and degradation of the polyimide coating of the restrictor capillary at the high temperature. Several solutions to the possible problems were examined: another cathode with permanent connections was used; the coating of the tip of the capillary tubing was burnt

off by the propane flame, followed by wiping out with acetone solution; leakage of the pump was tested. One of the pump parts was changed. The pump was flushed at a flow rate of 5 mL/min with HPLC grade ethanol for at least 30 minutes. The accuracy of the flow rate was tested by using a 10 mL graduated cylinder and a stopwatch. In this case, the signal stability was improved, and the effect of flashes was eliminated. A standard series of 0.5 %, 1 %, 2.5 % and 5 % glucose solutions was used to make the calibration curve for quantitative analysis. The optimal gas flows were the same as mentioned above. Detection limit was ~1% glucose solution. However, the reproducibility was poor. Irregular shape (multi-shoulders) of glucose peaks was still observed.

3.4 Conclusions

The modified FID was used for optimization of FID parameters. Two different cathode configurations were tested under the same conditions as in the previous section. Significantly improved signal stability was obtained by positioning the restrictor beside the FID jet via the cathode. The effect of FID parameters was studied by FIA of a standard series of 0.5%, 1%, 2.5% and 5% glucose solutions. The best performance was obtained, when hydrogen and oxygen flow rates were 130 mL/min and 115 mL/min, respectively. The water flow rate was set at 0.7 mL/min.

Chapter 4 – Optimization of the Modified FID System (II)

4.1 Introduction

In the project, the modifications were aimed at increasing the evaporation rate of the aqueous phase delivered to the FID flame. The FID performance was tested first with a conventional FID, followed by further studies of a modified FID using the same methods and setups as described in the previous chapters. During the detection, incomplete evaporation of the aqueous phase resulting in numerous problems was observed for all previous solutions. Based on the calculation of energy needed for the FID, 100 mL/min hydrogen flow for every 0.5 mL effluent flow out of the column was required to completely vaporize the effluent when the energy for vaporization was coming only from the flame. The main problem was that the residence time of water in the flame was very short for proper heat transfer for the vaporization process. In order to further reduce the amount of water passing through the flame of the FID while delivering all or most of the analytes to the flame, an alternative solution was tested. A modified FID equipped with an elongated burner was used to produce an elongated flame in order to increase the contact time between the aqueous filament and the flame. The influence of the shape of the flame on the sensitivity of the FID was evaluated using the same standard series of glucose solutions. Optimization of the FID parameters was initially performed at ambient temperature in flow injection mode. The FID sensitivity and linearity were studied.

4.2 Experimental Section

4.2.1 Chemicals and Materials

The same standard series of glucose solutions was used in the tests. A modified FID elongated burner, a shield, and a cathode collector were made in-house by the machine shop at the University of Waterloo. A rotameter calibrated for hydrogen used to

control the hydrogen flow was purchased from Cole Palmer Inc. (ON, Canada). Air or oxygen flow rates were adjusted using a digital GC flow meter (Agilent Technologies, Mississauga, ON, Canada).

4.2.2 Instrumentation

Modified FID Burner System

A modified FID burner schematically shown in **Figure 4-1** was mounted on a laboratory jack. The elongated burner was made of three major parts including two rectangular stainless steel plates (15 cm x 5 cm x 0.6 cm) and a sheet-like separator which was made of different materials (see later). The middle portion of the separator was cut away, placed between the two rectangular stainless steel plates and screwed tightly together creating a 10 cm long slit, which supported the elongated hydrogen-air flame (see **Figure 4-1**).

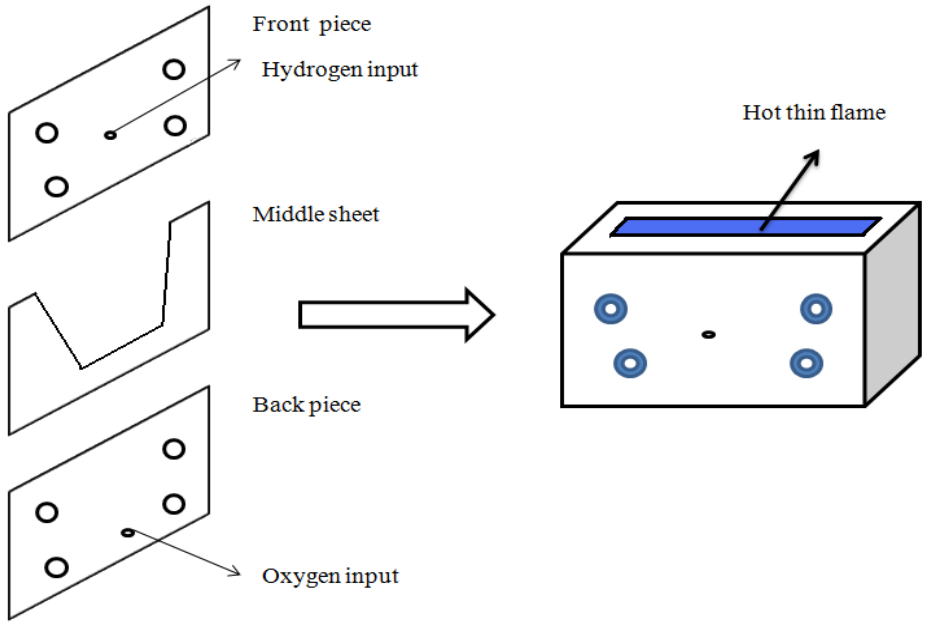

Figure 4-1: Modified FID burner

The modified cathode was made of a 15 cm long piece of stainless steel tubing. The front 10 cm portion of the tubing was split and bent into a U shape (see **Figure 4-2**). The other end of the tubing was connected to the FID amplifier in the GC, and was fixed in position (on the top or by sides of the flame) by a clamp. In order to avoid electronic short, a rectangular ceramic block was placed between the end of the tubing and the clamp. The other components of the system used were the same as those in the previous sections.

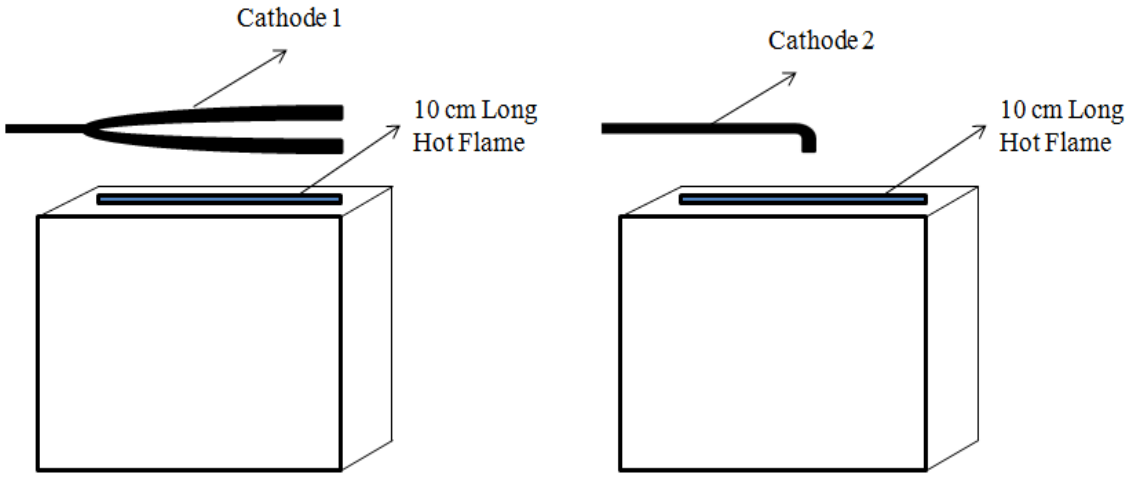

Figure 4-2: Two different modified cathodes

4.3 Results and Discussion

The Use of Different Separator Materials

Initial experiments were performed in flow injection mode at ambient temperature. The basic idea was to create a long hot flame as thin as possible. Different materials were used to make a thin separator between the two stainless steel plates as part of the FID elongated burner (see **Table 4-1**). The water flow rate was still set at 0.7 ml/min. A standard series of 0.5%, 1% and 2.5% (v/v) glucose solutions was injected sequentially at

time intervals of one minute and three times in each run. A hydrogen filter was used to filter hydrogen gas to remove any contaminants.

Table 4-1. Separator materials tested

Materials	Thickness
Stainless steel sheet 1	50 μm
Stainless steel sheet 2	20 μm
Teflon sheet	20 μm
PDMS sheet	20 μm

Hydrogen flow rate was the only factor changed at the early stages of the experiment. The baseline became noisy when the hydrogen flow rate was greater than 500 mL/min. With increasing hydrogen flow rate, the FID response increased, but the baseline became noisier. Different materials were tested for the separator. Because the high temperature of the burner could cause degradation of some materials such as Teflon and PDMS, stainless steel sheet metals were initially used. Both 50 and 20 μm thick stainless steel sheets were tested, but failed because of leakage of gas at the bottom of the FID burner. The same phenomenon was observed when using a PDMS sheet. Therefore, the Teflon sheet was used for further study. Degradation of the Teflon sheet at high temperature was not observed during the experiments.

Optimization of FID Parameters

As mentioned above, hydrogen flow rate was the only factor to be optimized. The effective range of hydrogen flow rate from 500 mL/min to 2.5 L/min was studied at the early stages of the analysis, since no signals were observed when hydrogen flow rates were lower than 500 mL/min. Moreover, hydrogen flow rates greater than 2.5 L/min resulted in flame instability. Because the digital flow meter could measure a maximum

flow rate of 1 L/min, a hydrogen rotameter was used instead. A needle valve was placed before the rotameter to control the hydrogen flow rate. Different positions of the cathode were tested. Cathode 1 was placed initially just above the FID elongated burner. The hydrogen flow rate was optimized for different positions of the cathode with respect to the surface of the burner. The best performance of the FID was obtained when the hydrogen flow rate was 2.3 L/min with the cathode positioned 1 centimeter above the FID burner. However, the baseline was very noisy. Tiny yellow flames spread over the whole flame zone were observed, and the middle part of the cathode turned red hot after some time. To avoid this effect, the cathode was positioned alongside the flame. The same result was observed as above. Many tiny yellow flames spread over the entire flame zone were observed when baseline tests were carried out at high hydrogen flow rate (up to 2.3 L/min). This phenomenon could be caused by impurity of the hydrogen gas at high hydrogen gas flows. Another reason was that sputtering resulted in different vaporization rates of the effluent in the flame, since the effluent droplets reached the flame at different times. In order to further consider the reasons, the entire length of the flame was divided into ten parts, which were tested individually.

Initially, a simple cathode 2 was made of a stainless steel tube which was bent at a 90 degree angle (see **Figure 4-2)**. Each 1 cm length of the flame from the left to the right of the entire 10 cm long flame was tested by placing the head of the cathode 1 cm above the surface of the elongated burner. The hydrogen flow rate was set at 2.3 L/min. The solution of 0.5% (v/v) glucose standard was used in the experiment. The best analyte signals were observed in the middle zone of the flame, but they were accompanied by high levels of noise. The signal could not be detected away from the middle of the flame. No significant differences were observed between the FID performance when using cathode 1 and partial flame test using cathode 2 in the middle zone of the flame.

To reduce the potential effect of air currents, a shield was made to cover the entire FID burner. Both right and left sides of the shield were the same height as the FID burner to avoid obstructing the cathode and the liquid filament of the effluent. The top of the shield was covered by a piece of folded aluminum foil. Optimization of the FID parameters such as hydrogen and water flow rates was carried out at ambient temperature for this setup. Based on the previous study, the hydrogen flow rate was optimized in the range from 1 L/min to 2.5 L/min. The water flow rate was set initially at 0.6 mL/min and increased to 1 mL/min. Solutions of 0.5 % and 1 % glucose standards were used in this experiment. Other settings were the same. Better FID sensitivity was observed in the experiments. However, the shape of the sample peaks was still irregular. Also, poor FID linearity was observed. The best FID performance was obtained when hydrogen as the only factor for gas flow was optimized at flow rate of 2.3 L/min. (see **Figure 4-3)**.

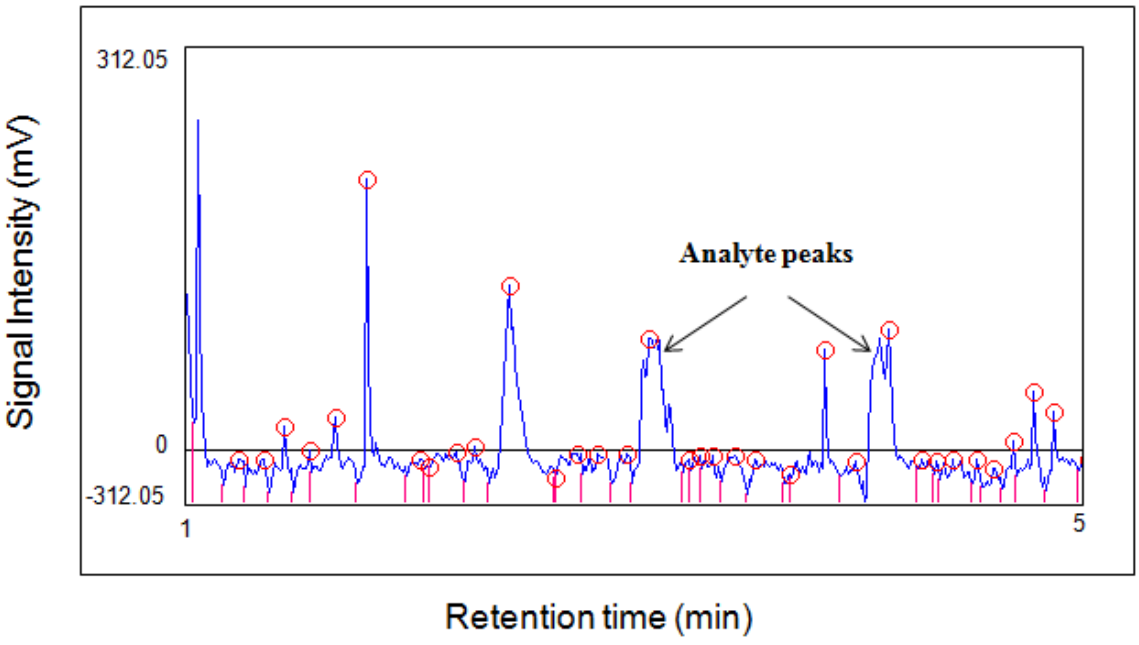

Figure 4-3 The best FID performance

In order to further increase the evaporation rate of the effluent in the flame, oxygen was used to generate a hotter flame. Another needle valve was used to control oxygen

flow. The oxygen flow rate was measured by a digital flow meter. Cathode 1 was used. Hydrogen and oxygen flow rates were first tested to find the optimal ratio at the lowest limit of hydrogen and oxygen flow rates, since the hydrogen flow rate was limited by the hydrogen rotameter. Initially, hydrogen and oxygen flow rates were set at 468 mL/min and 930 mL /min in the ratio of 1:2. The other settings such as water flow rate and glucose standards were kept the same as those in the previous experiments. With increasing hydrogen flow, better results were observed. The optimal ratio of hydrogen and oxygen flow rates was 1:1. Both flow rates were optimized in the range from 468 mL/min to 1.5 L/min. Because of the limit (maximum 1 L/min) of the digital flow meter, the hydrogen flow was split and measured by two identical flow meters. They were connected to two ends of a T-union, which was linked to the hydrogen gas tubing first after the needle valve. However, the best performance of FID was not better than that observed when hydrogen as the only factor for gas flow was optimized at flow rate of 2.3 L/min with air as the oxidant in the previous experiments.

Increasing water flow resulted in poor signals or even no signals. Decreasing the water flow also resulted in FID instability due to the effect of sputtering. An alternative solution was used to split the liquid effluent. The liquid effluent was split by a T-union which was linked to two pieces of capillary tubing of the same size and length. A clamp was used to fix the position of the two capillary tubes in order to generate two parallel liquid filaments from the effluent. In order to create a thin liquid filament at the lowest flow rate, different sizes of capillary tubing were tested. Two 40 μm I.D. capillary tubes were used. The smaller I.D. capillary tubing resulted in very high back-pressure (larger than 6000 psi), which exceeded the maximum pressure for the LC pump. Also, poor sensitivity and reproducibility were observed. Capillary tubing blockage occurred after a

few runs. The peak shape problem was still detected as mentioned in the previous section. Therefore, this method was discontinued for further study.

4.4 Conclusions

The new modified FID elongated burner was assembled using different separator sheets. The Teflon sheet (15 cm x 6cm, 20 μm thickness) proved to perform best and was used in the further study. A series of improvements was carried out due to the incomplete evaporation of the effluent. The best performance of the FID was obtained when the hydrogen flow rate was adjusted only, and set at 2.3 L/min.

Chapter 5 – Simplex Optimization

5.1 Introduction

In this project, the goal was to optimize the HPLC-FID coupling system by changing four selected parameters and by evaluating the effect of these parameters on the FID response. A series of different improvements were investigated using one factor at a time method in previous sections. However, this method failed to evaluate the influence of interactions in a multivariate system. A more efficient and practical optimization design is essential. With insufficient information about the true optimum region, the exact relationship between the response and the factors was not of primary interest. Sequential optimization was preferred to factorial designs. In this case, four-factor simplex optimization was carried out in the current setup.

5.2 Experimental Section

A solution of 0.5% glucose in deionised water was used for simplex optimization procedure. The FID set-up and all settings were the same as in Chapter 4. Rotameters were used to measure the flows of both oxygen and hydrogen (Cole Palmer, Canada). Cathode 1 was used and set at 1 cm above the surface of the FID elongated burner. The liquid filament from the outlet of the capillary tubing was delivered from the left side of the flame, and positioned about 0.5 cm above the surface of the FID burner.

Calculations for the Initial Simplex

In this project, the modified simplex method was used. To establish the first simplex in the series, it was necessary to decide upon the initial values for each of the factors and their ranges based on the previous study in Chapter 4. The step size that would result in a sufficiently large change in FID response was determined by using the

one factor at a time method in preliminary experiments. The initial simplex was located by calculating the coordinates of factors at each vertex based on the values shown in **Table 1-7**. In this case, four-factor simplex required vertices 1 to 5.

Initially, relatively large step sizes for the four factors were chosen in order to decrease the effort required to reach the general region of the maximum, but a smaller step size was used to increase the resolution when finding its exact position. The large step sizes of factors (A, B, C and D) are listed in **Table 5-1**. The initial values of the factors are shown in the first row of **Table 5-2**. The calculation for the coordinates of the initial simplex is shown below.

Table 5-1. The values of step sizes for four factors

Factor	Step Size For Part 1	Unit
Water flow rate (A)	0.1	mL/min
Hydrogen flow rate (B)	2	reading scale from the rotameter
Oxygen flow rate (C)	5	reading scale from the rotameter
Position of cathode (D)	2	cm

Sample Calculation for the coordinates of the initial simplex:

For Factor A, the initial value was 0.7 mL/min; Vertex No.2 was 1.000, and step size was 0.1 mL/min.

The second coordinate = 0.7 + 1.000 x 0.1 =0.8 (mL/min)

Calculations for Simplex Reflection

After the first simplex run, the worst experimental value (FID response) was eliminated. The coordinates for the new point were found by a simple calculation. First, the coordinates of the retained vertices were tabulated, and then the sum of each factor

was multiplied by 2/k (k was the number of the retained vertices). Finally, the coordinates of the discarded vertex were subtracted to obtain the coordinates for the new point. The new coordinates are shown in **Table 5-2**.

Table 5-2. Coordinates for Simplex Reflection

	Vertex No.	Factor A	B	C	D
k retained vertices	1	0.7	12	30	5
	2	0.8	12	30	5
	3	0.75	13.7	30	5
	4	0.75	12.6	34.1	5
Sum of retained coordinates……..		3	50.3	124.1	20
2/k * (sum)……..		1.5	25.15	62.05	10
Coordinates of discarded vertex….		0.75	12.6	31	6.6
Coordinates of new vertex……..		0.75	12.6	31.1	3.4

5.3 Results and Discussion

Precision of the measurement system

First, estimation of the reproducibility of the FID response was tested based on the same system and settings used in Chapter 4. The precision experiment (the first of the simplex procedure) was carried out four times before initialization of the optimization procedure. No significant change of the FID responses (peak area and S/N) from initially estimated value was observed during the optimization.

Simplex procedure

Four factor simplex optimization of the HPLC-FID coupling was carried out in FIA-FID mode. The simple optimization procedure started with five initial experiments in order to establish the practical range of factors and the corresponding FID responses. Four

major factors selected for the optimization were the position of the cathode, as well as hydrogen, oxygen and water flow rates. It should be mentioned here that the ranges of the values of the factors (**Table 5-3**) were chosen after studying the optimization of the FID parameters based on the FID setup used in Chapter 4.

In addition, the range of gas flow rate measurements was limited by the digital flow meters for both oxygen and hydrogen. Therefore the simplex optimization of HPLC-FID coupling was divided into two parts that were tested with the different step sizes individually. In the first part, the simplex optimization was tested by using the relatively large step size in order to quickly reduce the practical range of selected variables. Two rotameters were used for the high hydrogen and oxygen flows. Based on the information obtained from the first part, the second simplex optimization was carried out by using a smaller step size (see **Table 5-3**) to achieve reliable and accurate optimal FID conditions.

Table 5-3. Practical Range of Selected Variables and Step size in Part 2

Variables	Range	Size of Step For Part 2
Hydrogen flow rate	0.45 – 1.5L/min	50 mL/min
Oxygen flow rate	0.45 – 1.5L/min	50 mL/min
Position of the cathode	3 – 7 cm	1 cm
Water flow rate	0.65 – 1mL/min	0.1 mL/min

Simplex procedure for part 1 as seen in Table 5-5, halted after 16 experiments when the vertices of the simplex were outside of the practical range.

Table 5-4. Simplex Procedure in Part 1

Expt. No.	A $_{Water}$ (mL/min)	B $_{Hydrogen}$	C $_{oxygen}$	D $_{position}$ (cm)	Signal Height (mV)
1	0.7	12	30	5	3.6
2	0.8	12	30	5	4.8
3	0.75	13.7	30	5	3.0
4	0.75	12.6	34.1	5	3.1
5	0.75	12.6	31	6.6	2.5
6	0.75	12.6	31.1	3.4	3.2
7	0.75	10.9	32.6	4.2	1.4
8	0.75	13.7	30	5	2.5
9	0.75	12.5	26.4	4.2	3.1
10	0.75	10.8	28.7	3.8	3.0
11	0.75	11.2	33.5	4.4	3.5
12	0.75	13	33.5	5.1	3.7
13	0.75	11.5	32.4	6.4	3.2
14	0.75	13.1	29.5	6.3	1.6
15	0.75	21.7	29.1	4.4	2.9
16	0.75	16.3	31.8	3.4	2.9

Table 5-5. Simplex Procedure in Part 2

Expt. No.	A $_{(Water)}$ (mL/min)	B $_{(Hydrogen)}$ (mL/min)	C$_{(oxygen)}$ (mL/min)	D$_{(position)}$ (cm)	Signal height (mV)
1	0.7	600	500	4	1.7
2	0.8	600	500	4	1.2
3	0.75	643	500	4	1.6
4	0.75	614	541	4	2.4
5	0.75	614	510	4.8	2.3
6	0.68	636	526	4.4	3.4
7	0.69	589	539	4.6	3.1
8	0.74	627	558	4.9	2.9
9	0.68	619	572	4.2	4.3
10	0.65	622	557	5.1	3.0
11	0.61	606	539	4.3	2.9
12	0.62	653	558	4.4	4.2
13	0.71	659	568	4.8	4.5
14	0.70	662	573	4.6	3.1
15	0.68	661	610	4.6	3.3
16	0.65	634	581	4.4	3.2
17	0.65	622	530	4.3	3.1

After 17 experiments, the cessation of progress was verified since the simplex started to circle the maximum. As the simplex proceeded, vertex 13 gave the maximum FID response. However, detector performance under these conditions was actually slightly worse compared to that obtained earlier with the same FID setup when hydrogen/air mixture was used and the hydrogen flow rate was set at 2.3 L/min; both the signal and peak area were slightly lower at vertex 13.

5.4 Conclusions

For the proposed FID system of HPLC-FID coupling in the flow injection mode at ambient temperature, the simplex technique has been shown to be a straightforward and time effective procedure for optimization of four parameters. The best performance was obtained when the values of the four factors were as shown for vertex 13 in **Table 5-5**.

Future Work

Various methods to improve the performance of the FIA-FID coupling have been studied. Unfortunately, incomplete evaporation of the aqueous phase was the most significant problem in this project. It resulted in numerous problems such as irregular peak shape, non-linearity, low reproducibility, etc. Therefore, for further study, the water flow rate should be of primary concern. A microconcentric nebulizer could be tested since it produces very small droplets which could be more efficiently evaporated in the FID flame.

Next, the coupling of FID with HPLC using superheated water as the mobile phase will be tested. The characteristics of the HPLC-FID coupling will be examined. To minimize the thermal mismatch broadening, use of preheating is necessary, since temperature variations of the mobile phase along the column result in radial and axial temperature gradients, and therefore cancel all possible benefits in efficiency generated by the use of high temperatures. A stainless steel tube fitted with a metal block heater or a preheating coil could be used. The length of the preheating coil or the heated stainless steel tube will be chosen according to the water flow rate. Using a restrictor capillary before the FID will be required to prevent the evaporation of the eluent in the column. The capillary will be used to produce the liquid filament delivered to the flame.

Schematic diagram of the HPLC-FID system is shown in **Figure 6-1**. A stainless steel capillary (50 μm I.D.) will be placed between the column outlet and the FID system. PRP-1 column will be used as one of the most thermally stable stationary phases.

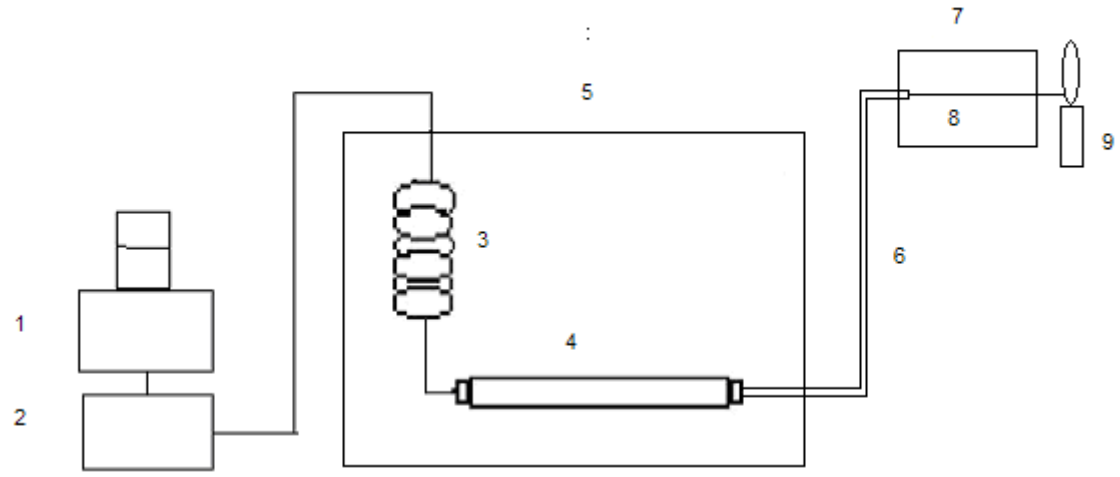

Figure 6-1. Schematic diagram of the HPLC-FID system proposed. 1 - degasser, 2 - pump with injection valve, 3 - preheating coil, 4 - column, 5 - column oven, 6 - restrictor, 7 - optional oven, 8 - liquid filament, 9 - FID.

References

1. Harris, D.C., "Quantitative Chemical Analysis", New York: W.H. Freeman and Company, 2007.
2. http://www.comsol.com/stories/waters_corp_hplc_systems/full/
3. Webster, G.K.; Jensen, J.S.; Diaz, A.R., J. Chromatogr. Sci. 2004, 42:484-490.
4. Young, C.S.; Dolan, J.W., LCGC 2003, 21:120.
5. Bin, Z.; Xiao F. L.; Bing Y., Anal. Bioanal. Chem. 2008, 390: 299-30.
6. Brunelli, C.; Gorecki, T.; Zhao, Y.; Sandra, P., Anal. Chem. 2007, 79:2472-2482.
7. Shi, H.; Taylor, L.T.; Fujinari, E.M., J. Chromatogr. A 1997, 757:183-191.
8. Lingeman, H.; Underberg, W.J.M.; eds. "Detection-oriented derivatization techniques in liquid Chromatography", New York: Marcel Dekker, 1990.
9. Vestal, M.L.; Fergusson, G.J., Anal. Chem. 1985, 557:2373-2378.
10. Yamashita, M.; Fenn, J.B., J. Phys. Chem. 1984, 88: 4451-4453.
11. Yamashita, M.; Fenn, J.B., J. Phys. Chem. 1984, 88: 4671-4681.
12. Singh, G.; Gutierrez, A.; Xu, K.; Blair, I.A., Anal. Chem. 2000, 72: 3007-3013.
13. Dolan, J.W., LCGC 2002, 20:524.
14. Hartonen, K.; Riekkola, M.L., Trend in Anal. Chem. 2008, 27:1-14.
15. Miller, D.J.; Hawthorne, S.B.; Gizir A.M.; Clifford, A.A., J. Chem. Eng. Data 1998, 43:1043.
16. Smith, R.M.; Burgess, R.J.; Chienthavorn, O.; Bone, J.R., LCGC North America 1999, 17:938-945.
17. Edge, A.M.; Shillingford, S.; Smith, C.; Payne, R.; Wilson, I.D., J. Chromatogra. A. 2006, 1132:206-210.

18. Takeuchi,T.; Watanabe, Y.; Ishii, D., J. High Res. Chromatogr. 1981, 4:300-302.

19. Claessens, H.A.; van Straten, M.A., J. Chromatogr. A. 2004, 1060:23-41.

20. Vanhoenacker, G.; Sandra, P., J. Sep. Sci. 2006, 29:1822-1835.

21. Lippert, J.A.; Johnson, T.M.; Lloyd, J.B.; Smith, J.P.; Johnson, B.T.; Furlow, J.; Proctor, A.; Marin, S.J., J. Sep. Sci. 2007, 30:1141.

22. Wyndham, K.D.; O'Gara, J.E.; Walter, T.H.; Glose, K.H.; Lawrence, N.L.; Alden, B.A.; Izzo, G.S.; Hudalla, C.J.; Iraneta, P.C., Anal. Chem. 2003, 75:6781.

23. Wilson, I.D., Chromatographia 2000, 52:S28-S34.

24. He, P.; Yang, Y., J. Chromatogr. A. 2003, 989:55-63.

25. Li, J.W.; Hu, Y.; Carr, P.W., Anal. Chem. 1997, 69:3884-3888.

26. Wu, N.J.; Tang, Q.L.; Lippert, J.A.; Lee, M.L., J. Microcol. Sep. 2001, 13:41-47.

27. Marin, S.J.; John, B.A.; Felix, W.D.; Clark, J., J. Chromatogr. A. 2004, 1030:255-262.

28. John V. Hinshaw. LCGC North America 2005, 23 Issue 12

29. Privett, O.S.; Erdahl, W.L., Anal. Biochem. 1978, 84:449.

30. Lapidus, B.M.; Karmen, A., J. Chromatogr. Sci. 1972, 10:103-106.

31. Karmen, A., J. Sep. Sci. 1967, 2:387-397.

32. Dubsky, H., J. Chromatogr. 1972, 71:395-399.

33. Guillemin, C.L.; Millet, J.L.; Dubois, J., J. High Resolut. Chromatogr. 1981, 4:280.

34. Miller, D.J.; Hawthorne, S.B., Anal. Chem. 1997, 69:623-627.

35. Ingelse, B.A.; Janssen, H.G.; Cramers, C.A., J. High Resolut, Chromatogr. 1998, 21:613.

36. Yang, Y.; Jones, A.D.; Mathis, J.A.; Francis, M.A., J. Chromatogr. A . 2002, 942:231-236.

37. Yarita, T.; Nakajima, R.; Otsuka, S.; Ihara, T.; Takatsu, A.; Shibukawa, M., J. Chromatogr. A 2002, 976:387.

38. Guillarme, D.; Heinisch, S.; Gauvrit, J.Y.; Lanteri, P.; Rocca, J.L., J. Chromatogr. A 2005, 1078:22-27.

39. Hooijschuur, E.W.J.; Kientz, C.E.; Th. Brinkman, U.A., J. High Resolut. Chromatogr. 2000, 23:309.

40. Smith, R.M.; Young, E.; Bone, J.R., HPLC 2007 abstract book, Ghent, Belgium P12.01.

41. Richard, G.B. "Applied chemometrics for scientists", J.Wiley & Sons Ltd. 2007.

42. Deming, S.N.; Morgan, S.L., Anal. Chem. 1973, 45:278A.

43. Duane, E. L., Anal. Chim. Acta, 1969, 46:193-206.